Materials Today Physics 22 (2022) 100613

Contents lists available at ScienceDirect

Materials Today Physics

journal homepage: https://www.journals.elsevier.com/materials-today-physics

Review of thermal transport in phononic crystals

Masahiro Nomura [a, b, *], Roman Anufriev [a], Zhongwei Zhang [a], Jeremie Maire [c], Yangyu Guo [a], Ryoto Yanagisawa [a], Sebastian Volz [a, d]

[a] Institute of Industrial Science, The University of Tokyo, Tokyo, 153-8505, Japan
[b] Research Center for Advanced Science and Technology, The University of Tokyo, Tokyo, 153-8904, Japan
[c] I2M, UMR 5295, CNRS-UB-ENSAM, 33 405, Talence, France
[d] LIMMS, CNRS-IIS IRL 2820, The University of Tokyo, Tokyo, 153-8505, Japan

ARTICLE INFO

Article history:
Received 5 November 2021
Received in revised form
21 December 2021
Accepted 12 January 2022
Available online 18 January 2022

Keywords:
Phonon
Phononic crystal
Thermal conductivity
Thermal transport
Thermoelectrics

ABSTRACT

Thermal transport at the nanoscale level is attracting attention not only because of its physically interesting features such as the peculiar behavior of phonons due to their pronounced ballistic and wave-like properties but also because of its potential applications in alleviating heat dissipation problems in electronic and optical devices and thermoelectric energy harvesting. In the last quarter-century, researchers have elucidated the thermal transport properties of various nanostructured materials, including phononic crystals (PnCs): artificial periodic structures for phonons. PnCs are excellent platforms for investigating thermal transport owing to their well-defined structural parameters. In addition, it is interesting to control thermal transport by interference, as demonstrated in the low-frequency regime with elastic waves and sounds. In this article, we focus on high-frequency phonons and review the thermal transport in semiconductor PnCs. This comprehensive review provides an understanding of recent studies and trends, organized as theoretical and experimental, in terms of the quasiparticle and wave aspects.

1. Introduction

A phonon is a collective excitation in condensed matter, which is a quantization of the vibration mode in elastic structures. Although phonons are not as popular as photons or electrons, they are ubiquitous in our daily lives. Phonons have a broad spectrum and are labeled in different frequency ranges as sound waves ($10–10^4$ Hz), ultrasound ($10^4–10^8$ Hz), hypersound ($10^8–10^{11}$ Hz), and heat (over 10^{11} Hz). Phonons in the lower frequency range are often excited electrically in the GHz range and are used in various applications, including musical instruments, measurements, sensing, imaging, and piezoelectric transducers. Micro- or nano-electromechanical systems, known as MEMS/NEMS, are exemplary applications of well-defined phonons generated in artificial mechanical structures [1,2]. In the very-high-frequency range, although the boundary is unclear, the thermal vibrations of atoms or molecules are the sources of phonons, called thermal phonons.

It is challenging and interesting to pursue the possibility of reducing or increasing the thermal conductivity by nanostructuring. The phonon propagation can be engineered by using phononic crystals (PnCs)—artificial materials with a periodic structure—for phonon interference owing to the induced periodicity. PnCs are often used to investigate or control sound waves, acoustic waves, and even heat transfer in solids. There are many insightful books and reviews on phonon transport in PnCs in various frequency ranges [3–8]; we focus on PnCs in the thermal spectral range in this review.

Fig. 1 shows an increasing number of articles on PnCs and thermal transport in PnCs, published since 2005. The percentage of articles on thermal transport in terms of the articles on PnCs also shows an increasing trend. The dimensions of PnCs used for heat conduction engineering are typically at the scale of the thermal phonon mean free path (MFP), the average distance between the scatterings, or the thermal phonon wavelength depending on the phenomenon of interest. Fig. 2 shows the different types of PnC structures for thermal transport studies in the incoherent and coherent regimes.

In the incoherent thermal transport regime, materials with high thermal conductivity and established process technologies, such as

* Corresponding author. Institute of Industrial Science, The University of Tokyo, Tokyo, 153-8505, Japan.
E-mail address: nomura@iis.u-tokyo.ac.jp (M. Nomura).

https://doi.org/10.1016/j.mtphys.2022.100613

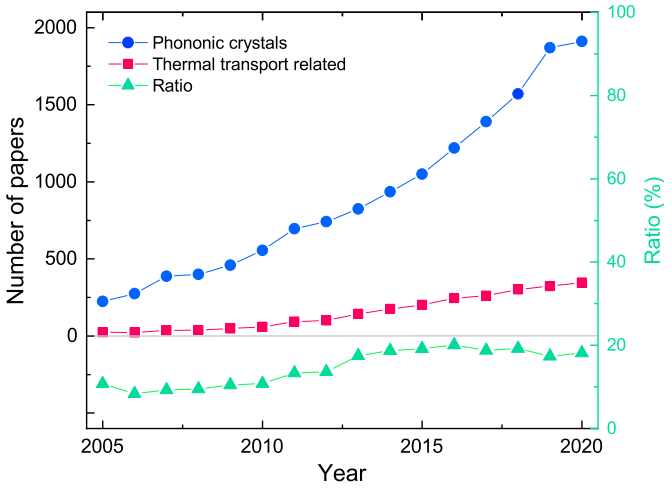

Fig. 1. Number of research articles indexed by Google Scholar each year. Investigations on phononic crystals (PnCs) (circles), thermal transport in PnCs (squares), and percentage of thermal transport studies on PnCs (triangles).

Si, are suitable for this study. The thermal phonon MFP in Si at room temperature is longer than a few hundred nanometers [11], which enables the use of PnCs with long periodicity to study thermal transport in the ballistic regime, as illustrated in Fig. 2(a). A large reduction in the thermal conductivity has been reported for various structures, including composite materials [12,13], nanowires [14,15], thin films [16,17], thin films with pillars [18,19], porous films [20–23], designed multilayered structures [24], and PnCs [25–28]. Such reduction of thermal conductivity is useful for applications related to thermoelectrics and thermal insulation. Several reviews on this topic have been published in the last two decades [29–34]. In addition, a recently proposed concept of ray phononics shows that heat flux engineering opens new possibilities for thermal engineering in solids by using ballistic transport of thermal phonons [9,35].

In the coherent thermal transport regime, the thermal transport is discussed based on the wave nature of thermal phonons. In a PnC structure, the thermal transport is discussed with the modulated phonon band created by the band-folding effect due to the periodicity of the PnC structure [36]. A properly designed PnC forms a complete phononic bandgap and can partially stop thermal phonon transport. However, the effect is limited because the frequency of the bandgap is low, and its frequency range is too narrow for the broad thermal phonon spectrum. As long as coherence is preserved, a graded superlattice structure, as shown in Fig. 2(f), covers a broader spectral range and effectively impedes thermal transport. The periodicities of a PnC and thermal phonon wavelength are similar, and the roughness of the system is much smaller than the wavelength required to realize coherent thermal transport.

The simplest PnC structure is a periodic multilayered material, such as a superlattice (Fig. 2(d)), which has periodicity in one direction and is referred to as one-dimensional PnC (1D PnC). Epitaxial growth methods enable PnC nanostructures with period of a few nanometers, and the interface is extremely flat at the atomic layer level, which is essential for coherent phonon scattering [37]. 2D PnCs have also been applied in thermal transport engineering in the last decade. However, PnC structures are mainly fabricated by a top-down semiconductor process, which is generally limited to the size of tens of nanometers with a surface roughness of a few nanometers. Therefore, the experimental observations are acquired at low temperatures [38,39]. 3D PnCs are an attractive experimental option for phononics, mainly in the low-

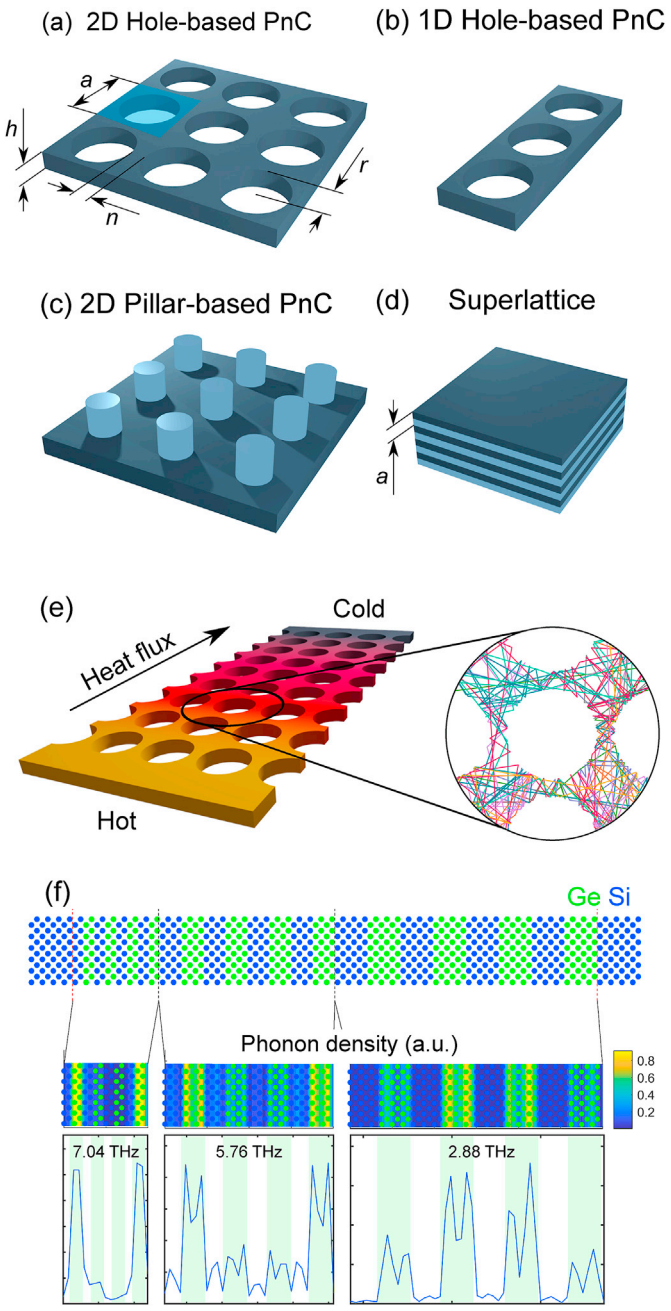

Fig. 2. (a–d) Schemes of PnCs of different types. (e) Illustration of a suspended 2D PnC structure with phonon trajectories (inset) in the incoherent regime [9]. (f) Simulation of a Si/Ge-graded superlattice with phonon localization in the coherent regime [10].

frequency range [40–42], but the studies in the high-frequency range, where the formation of fine structures is required, are mainly theoretical [43,44].

This review is divided into separate sections for incoherent and coherent thermal transport. In each section, recent theoretical and experimental studies on thermal transport in PnCs are reviewed in different subsections. Section 2 describes the incoherent thermal transport based on the quasiparticle nature of phonons. Most of the experimental studies on nanoscale thermal transport are in the incoherent regime. Thermal transport is discussed with the MFP of thermal phonons, which is an important characteristic of the transport and is determined by the limiting dimensions of PnCs.

Thermoelectrics is a promising application in phonon engineering by nanostructuring. Thermoelectric devices with PnC nanostructures are then introduced. Section 3 describes the coherent thermal transport based on the wave nature of phonons. It has been theoretically investigated mainly in nanostructures or low-dimensional materials by using mesoscopic or microscopic theories or simulations. In contrast, there are a limited number of experimental studies because it is challenging to prepare and observe coherent thermal transport owing to the short coherence length of thermal phonons.

2. Incoherent thermal transport

This section summarizes the studies and applications of PnCs in the incoherent regime. First, we review the theoretical and numerical modeling of incoherent thermal transport in PnCs. Then, we provide a meta-analysis of experimental studies that demonstrate reduction in the thermal conductivity of PnCs. Finally, as an application of this reduction, we discuss the improved performance of PnC-based thermoelectric generators.

2.1. Theory and simulations

The incoherent limit of thermal transport in semiconductor PnCs can be described via the quasiparticle description of phonons. Thus, the kinetic theory approach, which is based on the Boltzmann transport equation (BTE) of phonons [45–47], represents a robust solution to the incoherent thermal transport over a wide range of time and size. The kinetic theory is a statistical physical approach describing the evolution of the phonon distribution function, which denotes the probability of finding phonons in the system of interest. In contrast, atomistic approaches, including molecular dynamics (MD) [48,49] and non-equilibrium Green's function (NEGF) methods [50,51], are usually limited to PnCs with small characteristic sizes, where both the incoherent and coherent natures of phonons are important, as discussed later in Section 3.1.

There are usually two ways to model the incoherent thermal transport based on phonon BTE: (1) the kinetic formula of thermal conductivity from BTE, and (2) the direct numerical solution of BTE. In the first method, the bulk phonon MFP in the kinetic formula is replaced by the effective MFP in the PnCs. The effective MFP due to nanostructuring can be determined by either 1) a phenomenological model based on Matthiessen's rule [52,53], or 2) more accurate free path sampling techniques [54,55]. In the second method, two categories of numerical schemes are available for the direct solution of BTE: 1) deterministic methods represented by the discrete-ordinate method (DOM) [56–58] and its derivatives [59]; 2) stochastic method, namely, the Monte Carlo (MC) method [60–63]. Deterministic methods solve the phonon BTE by directly discretizing the phonon distribution in terms of time, space, wave vector, and polarization. The MC method solves the phonon BTE by representing the distribution function via pseudo-particles and tracking the free flight and scattering of the pseudo-particles. From the numerical implementation point of view, MC has an advantage over DOM in treating the complicated boundaries in PnCs. In addition, MC has lower memory cost than the DOM in the sacrifice of computational time and efficiency, which is attributed to the particle representation of the high-dimensional phonon distribution function. The drawbacks related to efficiency and fluctuation in MC simulations have been addressed by the recent development of variance-reduced deviational schemes [64,65]. Therefore, the MC method is more popular and recommended for modeling incoherent thermal transport in PnCs.

The incoherent thermal transport in PnCs has been extensively investigated and is relatively well understood when compared with coherent or partially coherent transport. In the interest of brevity, we introduce the crucial modeling studies chronologically instead of listing all the relevant studies. An early classical study is the modeling of the lattice thermal conductivity of superlattices by solving the phonon BTE, which explains the experimental data favorably, albeit under some simplified assumptions [66]. In principle, the BTE is valid when the dominant phonon wavelength (or coherence length) is much smaller than the superlattice period, so that the quasiparticle picture works well [67]. Nonetheless, the accurate treatment of thermal transport across the heterogeneous interface in superlattices in BTE modeling remains an open question, despite some subsequent studies reported on this topic [68–70]. Most studies have focused on the simulation of the thermal transport in periodic porous PnCs. In the very early research [56,60], a crucial methodology development, namely, periodic heat flux boundary treatment, was introduced in both DOM and MC implementations. Such a periodic boundary is essential for significantly reducing the computational cost by considering only a periodic unit of the phononic nanostructure. In a later work [54], the BTE model with the free path sampling technique and first-principle phonon properties provided a very accurate explanation of the experimental in-plane thermal conductivity of periodic nanoporous films. As the coherent thermal transport in nanoporous PnCs at elevated temperatures has been under debate, the MC simulation [63] revealed the importance of an amorphous oxide layer around the pores and the incoherent nature of thermal transport in Si nanomesh with a period of a few tens of nanometers between 100 K and 300 K. Indeed, to observe coherent thermal transport, very low temperatures and very smooth pore surfaces are required to preserve the phonon coherence throughout the PnC. In a very recent contribution [53], a theoretical model was developed based on the perturbation theory for phonon-surface scattering due to bond order deficiency and bond hardening, which is usually not taken into account. Thus, this theoretical model reproduced the measured ultra-low thermal conductivity of holey Si thin films with a period of 60 nm and a neck of approximately few tens of nanometers [53].

Theoretical models need to be further developed to describe the modified phonon MFP due to phonon-surface scattering in PnCs [52,62]. Because the computational cost of the direct numerical solution of phonon BTE remains appreciable, such a phenomenological model will be more efficient for practical engineering applications. In addition, as the hydrodynamic thermal transport in graphitic materials has attracted much attention in recent years [71–73], its manipulation via PnCs should be investigated in the near future. In terms of methodology, a direct solution of the phonon BTE under Callaway's dual relaxation model [74,75] represents a credible way to capture the effects of both normal and Umklapp scattering in this incoherent transport regime.

2.2. Experiments

Many experimental studies on PnCs relied on the quasiparticle picture of phonons. Indeed, because the phonon wave packets are essentially quasiparticles carrying heat, thermal transport can be viewed as the transport of phonon gas and it can be studied using properties native to particles. One such property is the phonon MFP. The MFP is linked to the thermal conductivity of the material and is generally proportional to its value. For example, in bulk Si, the MFPs of phonons at room temperature can be as long as tens of micrometers [76]. However, in thin Si membranes, scattering at the top and bottom surfaces shrinks this range manifold. In a 150-nm-thick membrane, the MFPs do not exceed a few hundred nanometers [77,78]. In PnCs, the MFP is further limited by the scattering on holes and can be reduced to several tens of nanometers [79].

Such a short MFP inevitably leads to low thermal conductivity.

Over the past decade, many studies have reported the thermal conductivity of PnCs. In this section, we show how the measured values of the thermal conductivity are linked to the MFP and fit into the larger picture of particle-like phonon transport. For consistency, we converted all the values reported in literature into effective thermal conductivity, which is the conductivity of the membrane of a given thickness. The effective thermal conductivity is given by $\kappa_{eff} = F \times \kappa$, where F is the volume reduction function and κ is the material thermal conductivity, which is the conductivity of the material between the holes. The volume reduction function F is often approximated using the Eucken formula $F = (1 - \varphi)/(1 + \varphi/2)$, where φ is the porosity [80]. For a typical PnC with a square lattice of holes, this approximation produces correct effective thermal conductivity within 5–10% of uncertainty, as demonstrated in supplementary materials of Ref. [81].

Fig. 3 shows the literature values of the effective thermal conductivity measured on Si PnCs at room temperature. To demonstrate a common trend, we plotted the data as a function of the neck size (n), which is the narrowest limiting dimension of PnCs. The literature data approximately follow the $\kappa \propto n$ trend. Remarkably, the different datasets follow a common trend regardless of the membrane thickness (h) or period (a) of the measured PnCs. The trend starts with the data for ultra-short PnCs by Yu et al. [25], Lim et al. [22], and Takahashi et al. [82]. In the middle range, this trend is formed by the data reported by Anufriev et al. [81,83] and Nakagawa et al. [84]. Finally, the data from Kim et al. [85] complete the trend over the long range. The trend suggests that the neck limits the phonon MFP more than any other dimension. In other words, most phonons are scattered at the narrowest region, that is, the neck, and the longest free path of the phonons is approximately set according to the neck width (n).

However, some studies [21,86,87] reported thermal conductivity values lower than the common trend. The lower values might be attributed to the high surface roughness of the holes in these studies. Indeed, the high surface roughness was linked to the reduction of thermal conductivity below the Casimir limit [88,89] and thus below the values observed for identical PnCs with smooth holes [90]. Moreover, Takahashi et al. [82] recently demonstrated that in PnCs with neck below 100 nm, the Young's modulus of the material decreases in the narrow regions. Such change in material properties may also reduce the thermal conductivity.

Because surface scattering dominates phonon transport, several studies have reasoned that the ratio of surface area to volume of the structure should be an important metric. Experiments and simulations have demonstrated that the measured thermal conductivity is indeed proportional to the surface-to-volume ratio [83,91–93]. However, when the neck becomes relatively small, its effect on the thermal conductivity dominates that of the surface-to-volume ratio [83]. Thus, thermal transport in PnCs is a complex phenomenon affected by the neck, surface roughness, surface-to-volume ratio, and even changes in Young's modulus.

In addition, the stochastic motion of phonons in PnCs may lead to an unexpected effect of directional phonon transport. Indeed, phonons are diffusely scattered on the hole surfaces in random directions, and the only way to escape the scattering is to pass between the holes. Hence, the phonon directions are constantly randomized by the scattering while the passage between the holes ensure that only phonons with selected directions can pass. Such a process of randomization and selection causes the initially random phonon gas to evolve into the directional flux of phonons [81,90,91]. This notion lays the foundation for the ray phononic concept [9], which enables the realization of phononic devices such as thermal lenses, guides, filters, and cloaks [9,81].

2.3. Application to thermoelectrics

Thermoelectrics is one of the most promising applications of PnCs. Thermoelectric devices have been used for power generation and electronic refrigeration. Currently, research is focused on enhancing the performance of thermoelectric materials (ZT) [94–97]. There are two main approaches to increasing the ZT values: material science and nanostructuring. The dimensionless figure of merit of thermoelectric material is given by

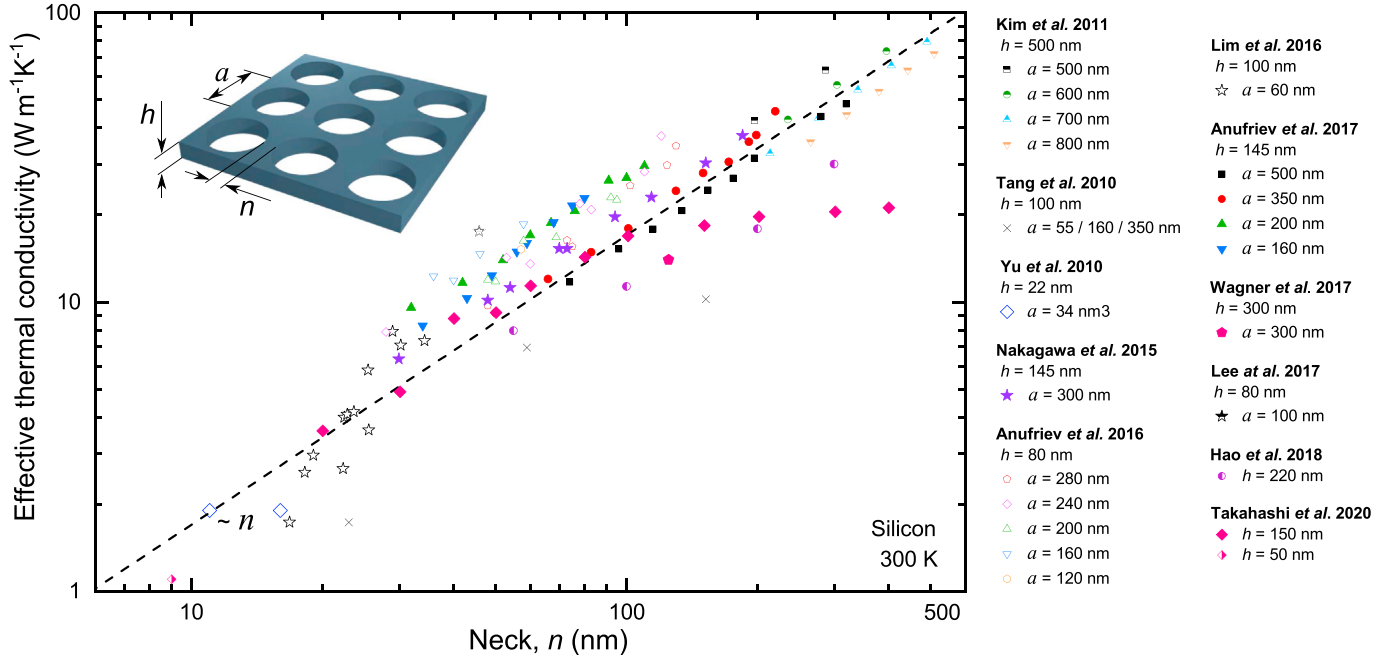

Fig. 3. Effective thermal conductivity of Si PnCs at room temperature as a function of neck size, reported in literature [21,22,25,81–87]. The data show a common trend, suggesting that the phonon MFP in PnCs is limited by the neck rather than any other dimension.

$$ZT = S^2\sigma T \Big/ (\kappa_{lat} + \kappa_{ele}), \quad (1)$$

where S is the Seebeck coefficient, σ is the electrical conductivity, T is the average temperature, and κ_{lat} and κ_{ele} are the thermal conductivities of the lattice and charge carriers, respectively. The material science approach focuses on finding materials with a large power factor, $S^2\sigma T$ [98–100]. However, the nanostructuring approach maximizes the value of σ/κ based on Slack's principle, known as "phonon-glass electron-crystal" [101]. This principle proposes the design of a material with high electrical conductivity, such as crystal, and low thermal conductivity, such as glass, for achieving larger ZT.

In addition to material design, top-down nanostructuring is also an effective method to increase the ZT value of materials with relatively long phonon MFPs. Because the lattice thermal conductivity is given by $\kappa_{lat} = C_v v \Lambda/3$, a material with high lattice thermal conductivity generally has long phonon MFPs, such as Si, SiC, AlN, and BAs [102–104]. Si is the most suitable material for forming nanostructures for thermal phonon engineering owing to the mature semiconductor process technology.

Many studies have reported reduced thermal conductivity in PnCs, as discussed in the previous section. The basic design rule of a PnC for thermoelectric applications is the Slack's principle [101], but this is applicable to artificial structures. The period and neck size of PnCs were chosen by considering the thermal phonon MFP spectrum of the material. At room temperature, most thermal phonons have MFPs between 10 nm and 1 μm in single-crystalline Si [11], and shorter than a few hundreds of nanometers in a thin film (~ 100 nm thick) because of phonon scattering at the surface [77]. The MFP of charge carriers in heavily doped Si does not exceed tens of nanometers [105], which is much shorter than that of thermal phonons. The difference in the MFP ranges of charge and heat carriers allows the application of Slack's principle by taking the periodicity of a few hundreds of nanometers with a neck size of tens of nanometers. The MFP of thermal phonons becomes much shorter owing to the scattering on holes, but the MFP of the charge carriers remains almost the same. As a result, σ/κ is increased in the PnC nanostructures, leading to larger ZT.

PnC nanostructures are good platform for investigating the enhancement of thermoelectric performance by nanostructuring owing to their well-defined structural parameters. There are many experimental reports on the large reduction in thermal conductivity of nanostructured Si, including PnC nanostructures, for the purposes of fundamental phonon transport study and thermoelectrics [14,22,25,79,106–112]. El-Kady et al. conducted an experimental study on the enhancement of the ZT of single-crystalline Si films (500 nm thick) with PnC nanostructures. They demonstrated a systematic reduction in thermal conductivity by changing the radius of the circular holes [27]. They also demonstrated that ZT was enhanced by a factor of 1.4 in a PnC with a = 700 nm and n = 213 nm when compared with that of an unpatterned film. Lim et al. fabricated PnCs in a 100-nm-thick Si film with dimensions of a ~ 60 nm and n ~ 20 nm by block copolymer lithography, and reported ZT ~ 0.04 with an extremely small k ~ 1 $Wm^{-1}K^{-1}$ at room temperature [22]. Liu et al. also fabricated PnCs in a 100-nm-thick Si film with n = 45 nm by electron beam lithography, and reported k ~ 6 $Wm^{-1}K^{-1}$ and ZT = 0.09 at room temperature [112].

Single-crystalline Si is better for fundamental studies on the phonon and heat transport phenomenon because of its long phonon MFP, but poly-Si is more suitable for thermoelectric applications. The grain boundary scatters the phonons more efficiently than charge carriers in heavily doped Si, which results in higher ZT. Nomura et al. fabricated PnC nanostructures in a suspended 145-nm-thick poly-Si thin film to investigate the effect of PnC nanostructuring on thermoelectric performance enhancement [108]. The PnCs are an array of circular holes aligned in a square lattice with a = 300 nm, and the electrical and thermal conductivities were measured for structures with various hole radii (Fig. 4 (a, b)). For both p- and n-doped Si, a large reduction in thermal conductivity was observed, whereas the electrical conductivity decreased slightly. Fig. 4 (c) shows the increasing trends of ZT with r, which indicates that the PnC nanopatterning is useful for ZT enhancement. The period of 300 nm of the PnC was chosen to follow Slack's principle, that is, shorter than the thermal phonon MFPs and longer than the MFPs of charge carriers. More precisely, the neck size is an intrinsically important parameter, which

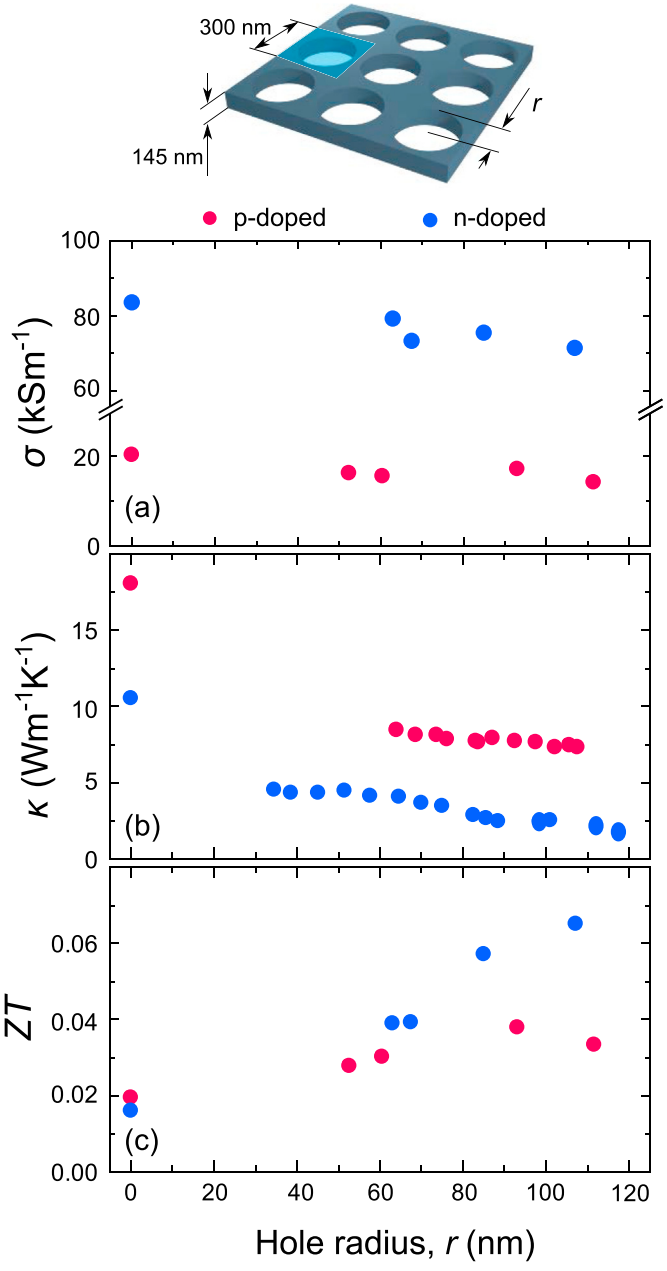

Fig. 4. Measured (a) electrical and (b) thermal conductivities of p- and n-doped poly-Si PnC nanostructures with various hole radii, and (c) calculated thermoelectric figure of merit [108].

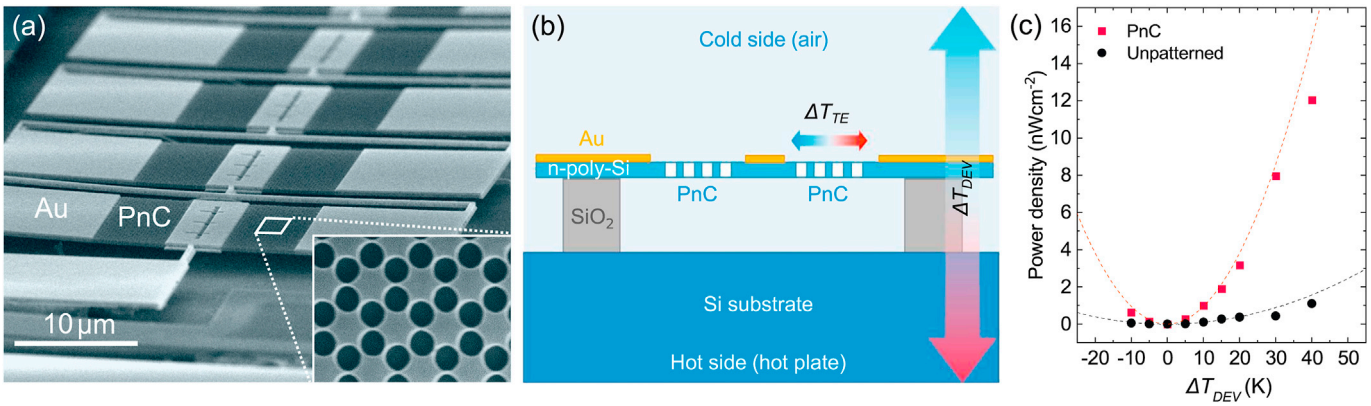

Fig. 5. Fabricated uni-leg planar-type Si thermoelectric generator with PnC nanostructures. (a) Scanning electron microscope (SEM) image. (b) Schematic of cross-sectional view of the device (c) Measured power density at various temperature differences between the hot and cold sides, ΔT_{DEV}, for the generator with (squares) and without (circles) PnC nanostructures [118].

determines the enhancement of *ZT*. However, we should be aware that the neck size should be kept longer than the MFPs of charge carriers to maintain the *ZT* enhancement.

In general, thermoelectric generators with Si thin films are planar, and can be fabricated using the CMOS-MEMS technology. Several studies have reported planar-type Si thermoelectric devices based on the standard CMOS process [113–119]. After conducting the proof of concept, uni-leg planar-type Si thermoelectric generators were fabricated, and the power densities of the devices with and without PnC nanostructures were compared. The structure is depicted in Fig. 5; the details of the device fabrication and structure can be found in our previous study [118]. The device was fabricated using a silicon-on-insulator wafer with a 300-nm-thick n-doped poly-Si thin film as the active layer. The output power densities were compared at various temperature differences (ΔT_{DEV}) between the cold side on the top (air) and the hot side (Si substrate) attached to a temperature-controlled stage. The PnC device showed a larger open-circuit voltage owing to a larger temperature difference in the thermoelectric film (ΔT_{TE}), as depicted in Fig. 5(b). The Seebeck coefficient was not changed by the nanopatterning at this scale. Finally, the output power density *P*, which is proportional to ΔT^2, was enhanced by a factor of ten (Fig. 5(c)). This result clarifies the advantage of PnC nanopatterning. However, there are some challenges to overcome to increase the performance. The most important issue is the thermal design of the device. The reason for the low *P* is the small ΔT_{TE}, which is only 0.2% of ΔT_{DEV}; in other words, the device generated electric power with ΔT_{TE} ~ 10 mK in this measurement. The thermal design of the device is as important as the material performance. Because planar-type thermoelectric devices are thin, a proper heat dissipation path at the cold side should be designed to realize a large ΔT_{TE}. We expect that the power generation capacity of this planar-type thermoelectric device will reach the order of 10 μWcm^{-2}K^{-2}, which will enable low-frequency intermittent sensing applications for the Internet of Things.

3. Coherent thermal transport

In this section, we summarize the most recent and important progress in the study of coherent thermal transport in PnCs through theoretical simulations and experiments. We first review the theoretical studies based on various theories, including BTE, NEGF, and MD simulations. The different influences on coherent thermal transport are specifically discussed, as reported through various theoretical analyses. Then, we discuss the most notable experimental realizations linked to the coherent thermal transport in PnCs. Specifically, we present the results of 1D and 2D hole- and pillar-based PnCs and superlattices, and finally highlight promising materials such as 2D materials and BAs.

3.1. Theory and simulations

When the period of the PnCs is comparable to the coherence length of the phonons [33,36,122–124], the thermal transport is dominated by the coherent phonons, which exhibit pronounced wave behavior. However, the coherence length of phonons is usually shorter than hundred nanometers [123,125], that is, typically at the atomistic scale or nanoscale. Therefore, the coherent thermal transport phenomena in PnCs have been widely studied in the nanostructures or low-dimensional materials [124,126–128] by using various mesoscopic or microscopic theories or simulations, including BTE, NEGF, and MD simulations. In this section, we summarize the state-of-the-art theoretical and simulation-based studies on coherent thermal transport.

3.1.1. Boltzmann transport equation

BTE is a widely used theory in the calculation of thermal conductivity by treating thermal phonons as quasiparticles [45,46,129]. As the wave nature of phonons is not explicitly included in the BTE, it cannot be directly used to model coherent thermal transport. Extensive effort has been devoted to fully capturing both the wave- and particle-like behavior of phonons within the BTE theory. Considering the effect of anharmonic scattering (represented by the phonon MFP Λ) on the coherent and incoherent transport regimes, Simkin and Mahan [130] proposed a phenomenological thermal conductivity model by adding an imaginary part i/Λ to the wave vector $\mathbf{k}$. Thus, this model demonstrated the minimum thermal conductivity with regard to the period length of the superlattices [130]. Nevertheless, this classical model needs to be further improved or developed for the following reasons: 1) other dephasing phonon scatterings are not considered, such as diffuse interface scattering; 2) the effect of the secondary periodicity of PnCs on the MFP is not properly included; and 3) the transition of thermal phonons from coherent to incoherent transport is more related to the coherence length than the MFP, as shown by some other studies [67,123,125,131].

Another way to capture the wave nature of phonons in BTE is to treat the PnCs (e.g., superlattices) as a new homogeneous material with the secondary periodic component (e.g., one period of superlattices) as a unit cell. The phonon properties (dispersion and

scattering rates) of the new material can be obtained via either first-principles (DFT) calculations [120,132] or MD simulations [133]. The DFT-BTE study [132] on infinitely long Si/Ge superlattices with perfect interfaces (Fig. 6(a)) shows a monotonous decrease in thermal conductivity with increasing period length (see inset in Fig. 6(c)), which is well consistent with the trend indicated by the pure coherent calculations [134,135], yet inconsistent with that observed in some experimental results [122,136,137]. With further consideration of the diffuse phonon-interface scattering, the cross-plane thermal conductivity of the superlattices shows the expected minimum thermal conductivity (Fig. 6c)) due to the competition between the low-frequency coherent phonons and the high-frequency phonons dephased by the interfacial roughness [120]. In such BTE models with redefined phonon modes, it remains a challenging task to accurately consider the effect of the finite size of the PnCs.

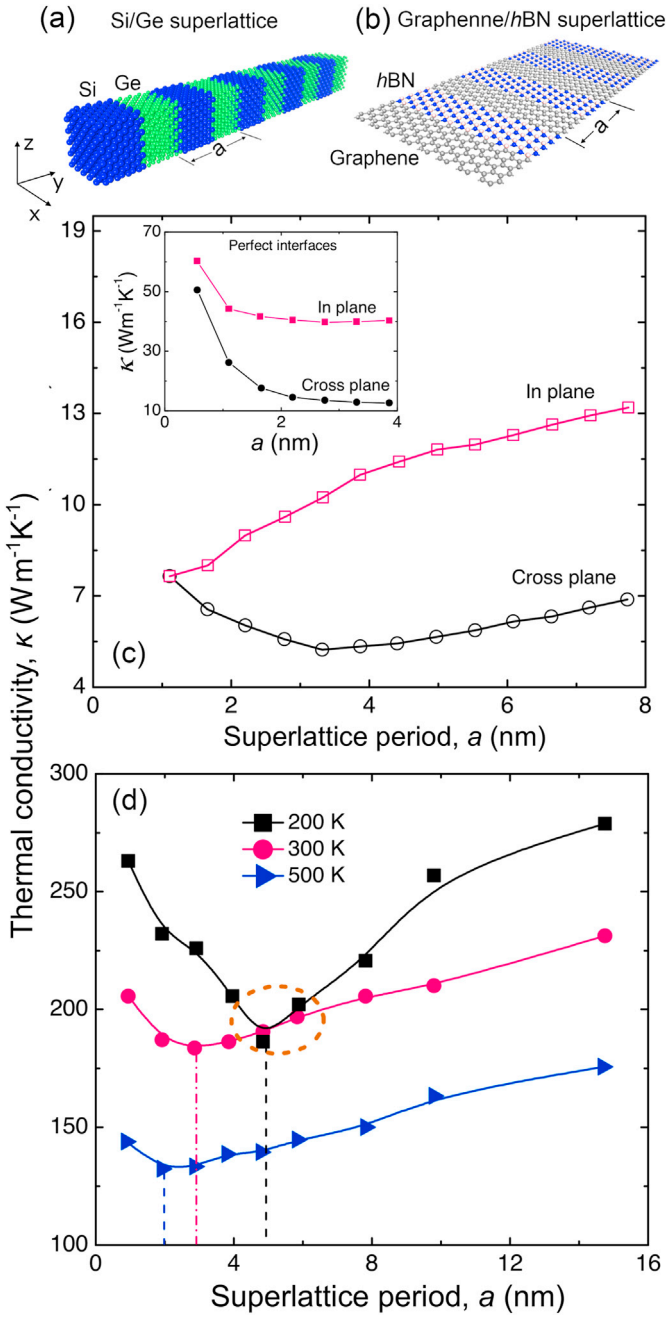

Fig. 6. Minimum thermal conductivity from simulations. Schematic of (a) Si/Ge superlattice and (b) graphene/*h*BN superlattice. (c) Thermal conductivity of Si/Ge superlattices with different interface roughness values versus period lengths. Reprinted with permission from Ref. [120]. Copyright (2013) American Physical Society. (d) Thermal conductivity of graphene/*h*BN superlattices versus period length under different temperatures. Reprinted from Ref. [121] with permission from AIP Publishing.

3.1.2. *Atomistic non-equilibrium Green's function*

By solving Heisenberg's quantum dynamic equation of atoms, the atomistic NEGF formalism inherently considers the wave nature of thermal phonons [138–140]. The linearly length-dependent thermal conductivity of the AlAs/GaAs superlattice is shown through NEGF calculations as the characteristic feature of the ballistic coherent transport of folded superlattice phonons, as observed in experimental measurements [141]. The increasing linear trend is weakened by the growing population of high-frequency incoherent phonons at elevated temperatures or by phonon dephasing due to interfacial roughness [141–143]. On the other hand, the observed length dependent thermal conductivity in Ref. [141] has also been contributed by the acoustic mismatch between the two different layers. However, the increased thermal conductivity at short period length in the further minimum thermal conductivity measurements in superlattices [122,137] clearly indicates the existence of coherent phonon as the acoustic mismatch situation is insensitive to the period length of two layers in the superlattices. In addition, the minimum thermal conductance has been reproduced by NEGF calculations in isotopic graphene superlattices [144] and graphene/*h*BN superlattices (Fig. 6(b)) [145]. These studies emphasize the role of diffuse interface scattering in the transition of heat transport from a coherent regime to an incoherent one. The consideration of another important decoherence mechanism, that is, anharmonic phonon-phonon scattering, in NEGF formalism can be performed in principle [51,146]; however, it remains challenging owing to computational limitations. It should be mentioned that these decoherence mechanisms can also suppress the coherent thermal transport phenomenon. As reported before, the minimum thermal conductivity is difficult to be experimentally observed, particularly at high temperatures or with rough interfaces [136,147].

The Anderson localization of thermal phonons, as an important phenomenon in the coherent wave regime [150], has also been studied in recent years through ballistic NEGF calculations. The maximum thermal conductivity according to system length was investigated for GaAs/AlAs superlattices with randomly embedded ErAs nanodots through NEGF simulation [151], which was later confirmed through experimental measurements [152]. This maximum represents a transition of heat transport from ballistic to localization regimes as the system length increases to become comparable to or larger than the localization length of the phonons. Further investigations also revealed that the localization behavior of thermal phonons is strongly mode dependent [148,151,152]. The aperiodic Si/Ge superlattices shown in Fig. 7(a), the ballistic modes, propagation modes, and localized modes coexist (Fig. 7(c)) but they are distributed in different phonon modes [148]. The onset frequencies of the localized modes have been shown to be more or less the frequency of the LA and TA branches near the boundary of the folded Brillouin zone. However, the exact relationship between the localization and coherence length (or wavelength) of the phonons in the full Brillouin zone remains an open question. In a recent study by Guo et al. [10], partial phonon localization was demonstrated in graded Si/Ge superlattices with moderate disorder. The minimum thermal conductivity according to system length was thus obtained owing to the competition between the localization and ballistic transport of folded phonons.

3.1.3. Molecular dynamic simulations

MD simulations model the classical dynamic evolution of atomic vibrations [48,153–155], where the wave nature of thermal phonons is inherently captured. Coherent thermal transport has been widely explored through MD simulations in 1D superlattices [156–159] as well as other 2D PnCs [121,123,149,160–164]. Because diverse scatterings are intrinsically included in the atomic structure and dynamic process, many influencing factors have been studied for coherent thermal transport in MD simulations. In particular, when compared with the preceding ballistic NEGF modeling, the unique effects of phonon-phonon scattering on coherent thermal transport have been uncovered. For example, the position of minimum thermal conductivity shifted to a shorter period length as the temperature increased (Fig. 6(d)) [121,149], due to the increasing decoherence effect of anharmonic scattering. Moreover, the suppressed coherence length from phonon-phonon scattering can result in a weak dependence of the minimum thermal conductivity on the system length [123].

The Anderson localization of phonons was also investigated by MD simulations in aperiodic Si/Ge superlattices (Fig. 7(a)) and aperiodic porous graphene PnCs (Fig. 7(b)) [131,149], which naturally consider the effect of anharmonicity neglected in ballistic NEGF. The influence of the disorder level on Anderson localization was studied in an aperiodic Si/Ge superlattice (Fig. 7(d)) [131]. A sufficient level of disorder is necessary to fully localize the phonon modes. For some phonon modes, partial localization appears owing to decoherence, and the transmission decays to a non-zero constant value with the system length (Fig. 7(c)) [10,131,149]. Owing to the rapid progress in computer science, many recent studies [165–169] have focused on the minimization of thermal conductivity by maximizing the Anderson localization for thermoelectric applications. By combining machine learning algorithms and MD simulations, the thermal conductivity in aperiodic PnCs can be further reduced up to 30% from the minimum thermal conductivity in the periodic case [165].

The wave nature of thermal phonons is also responsible for other interesting wave-related phenomena in phononic metamaterials, such as wave hybridization [18,19,170–174]. Pillar-based PnCs have been demonstrated as a platform for exploring the wave nature of thermal phonons through wave hybridization [8,18,171,174,175]. The wave hybridization between the pillar local resonances and the base is believed to result in a large reduction in the group velocity around the resonance modes, which has been asserted to be mainly responsible for the reduction in thermal conductivity in the atomic-scale pillared Si membrane [18]. A recent study reported that pillars can also suppress the phonon lifetime in pillared Si nanowires [176]. The difference might be caused by a different degree of hybridization or interaction between the base and pillars, which has a critical effect on thermal transport in pillared systems [177]. The underlying mechanisms and controversies of wave hybridization in pillar systems are very similar to those of thermal transport in host–guest systems [178–185]; thus, their connections should be explored in the future.

Because the MD simulation combines coherent and incoherent thermal transport, considerable effort has been made to decompose the total thermal conductivity into the contributions from these two components. A two-phonon model that relies on length-dependent thermal transport simulation was proposed [186]. Using this two-phonon model, Wang et al. [186] and Hu et al. [149] found that coherent phonons dominate the thermal transport in ordered nano-PnCs over a large length scale, whereas their contribution exponentially decays in disordered nano-PnCs due to localization.

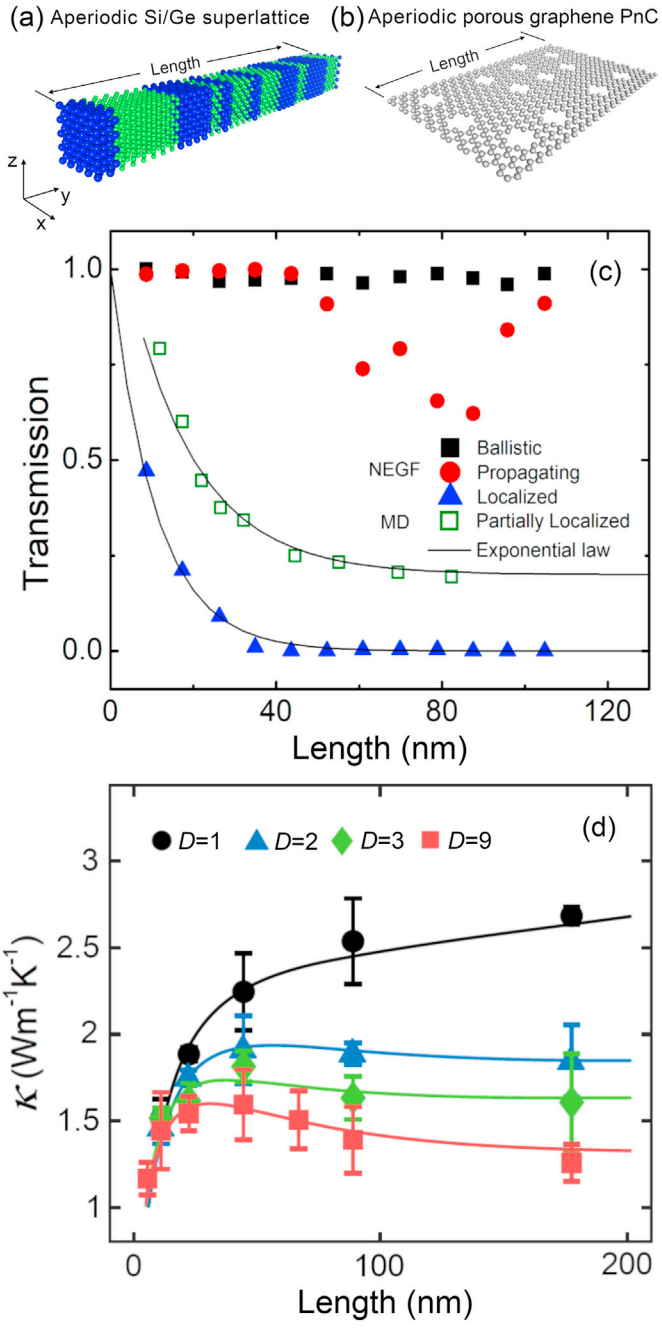

Fig. 7. Anderson localization in PnCs. Schematic of (a) aperiodic Si/Ge superlattice and (b) aperiodic porous graphene PnC. (c) Transmission of ballistic, propagating, localized, and partially localized modes in aperiodic PnCs. The NEGF results are from Ref. [148] for the aperiodic Si/Ge superlattices in (a). The MD results are from Ref. [149] for the aperiodic porous graphene PnCs in (b). (d) Maximum thermal conductivity versus length in aperiodic Si/Ge superlattices as the disorder increases. *D* represents the degree of disorder. Reprinted with permission from Ref. [131]. Copyright (2019) of the American Physical Society.

In some other studies [67,125,187], it was shown that it was difficult to distinguish the thermal phonons into coherent or incoherent groups, as they simultaneously constitute these two aspects, that is, in the form of wavepackets. Our recent study [187] showed that the temporal coherence of thermal phonons could be calculated from MD simulations, and its effect on thermal transport was estimated using a generalized phonon decay law.

3.2. Experiments

Experimental demonstration and use of coherent phonon scattering for thermal applications has been the overarching goal of PnC experiments but has remained challenging for the past decade owing to the stringent conditions required. Coherent thermal transport commonly refers to phonons displaying wave properties, such as interferences, Bragg and local resonances, and localization, as described in the previous sections. Such phenomena, largely observed in acoustic crystals at low frequencies or photonic crystals for photons, are detailed in the previous section from a theoretical perspective. They have encouraged the realization of several experiments to demonstrate their use in practical implementations. Although coherent thermal transport, which stems from elastic reflections of phonons from boundaries, can enable the blocking, enhancement, or guidance of thermal energy in specific directions, it requires that the phonon wavelength be much larger than the surface roughness, which is usually not satisfied for thermal wavelengths of a few nanometers at room temperature. Under these conditions, atomically flat interfaces or atomic-scale structures are typically required. Alternatively, experiments at low temperatures, at which phonon wavelengths drastically increase, have shown the impact of such coherent behavior of thermal transport. In this section, we introduce the experiments that have been realized to date with 1D and 2D holes and pillar-based PnCs and superlattices; some of the successful implementations are shown in Fig. 8. We also discuss the potential of novel materials such as SiC, BN, and BAs, in which phonons with longer MFPs contribute substantially to thermal transport.

3.2.1. Hole-based PnCs

PnCs exist in different types and aim to control the propagation of phonons by interference and modification of the dispersion relation due to the artificial periodicity. Apart from superlattices, which will be detailed later, most experimental realizations are one- or two-dimensional structures with a periodic arrangement of holes. In one-dimensional PnCs consisting of beams with arrays of holes with feature sizes of a few hundred nanometers, experiments and predictions at room temperature exclude the influence of coherent thermal transport [15]. Some models [39,188] suggest that coherence affects thermal transport below 10 K. Maire et al. [39] compared the thermal conductivity in identical beams with ordered and disordered arrays of holes (Fig. 8(d-e)). They observed that the thermal conductivity was 8% lower in the former at a temperature of 4 K and interpreted it as an indication of coherent thermal transport. Furthermore, this effect decreased with increasing temperature and disappeared above 10 K. A similar effect was observed for 2D PnCs in the same study under identical conditions, with the only difference being that holes in the ordered structure were positioned in a square lattice and disorder was introduced in two directions: along and perpendicular to the heat flow direction. Apart from this indirect observation, the only clear and quantitative measurements of coherent thermal transport in similar PnCs to date have been reported by Maasilta et al. [38,135] (Fig. 8(a)). They calculated the thermal conductance from the dispersion relation modified owing to the periodicity of the PnC, and showed that their measurements at ultra-low temperatures with superconducting junctions at the center of the PnCs (Fig. 8(a)) directly correlated with the calculation results. They observed that heat conduction is strongly suppressed in PnCs when compared with the unpatterned membrane owing to the combined changes in the phonon group velocity, density of states, and energy distribution. They showed that although the thermal conductance is reduced due to modifications in the band structure, the key parameters are the changes in the group velocity and density of states rather than the presence of potential bandgaps. Experiments for a wide range of PnC periods confirmed this; it was shown that these measurements were inconsistent with a predominantly incoherent thermal transport regime, as can be seen by the discrepancy between the measurements and simulations in Fig. 8(b). The non-monotonic trend observed with an increase in the period further suggests that they reach the crossover between coherent and incoherent thermal transport for sufficiently large periods, as shown in Fig. 8(b). This crossover, the mechanisms for which are explained in the previous sections, has been mainly observed in superlattices, as will be detailed in the following section.

3.2.2. Modulated beams and pillar-based structures

Hole-based PnCs introduce artificial periodicity by removing material; the alternative of adding periodic extensions or modulations to the existing structures has also been theoretically [191–195] as well as experimentally investigated. The first type of structure to be fabricated consisted of nanobeams with corrugation, that is, the periodic modulation of width. In these structures, the experimental results for a wide range of temperatures can be explained by surface scattering, even down to 4 K [196] and sub-Kelvin temperatures [197]. Indeed, the reduced thermal conductivity is explained by a reduction in the MFP of phonons stemming

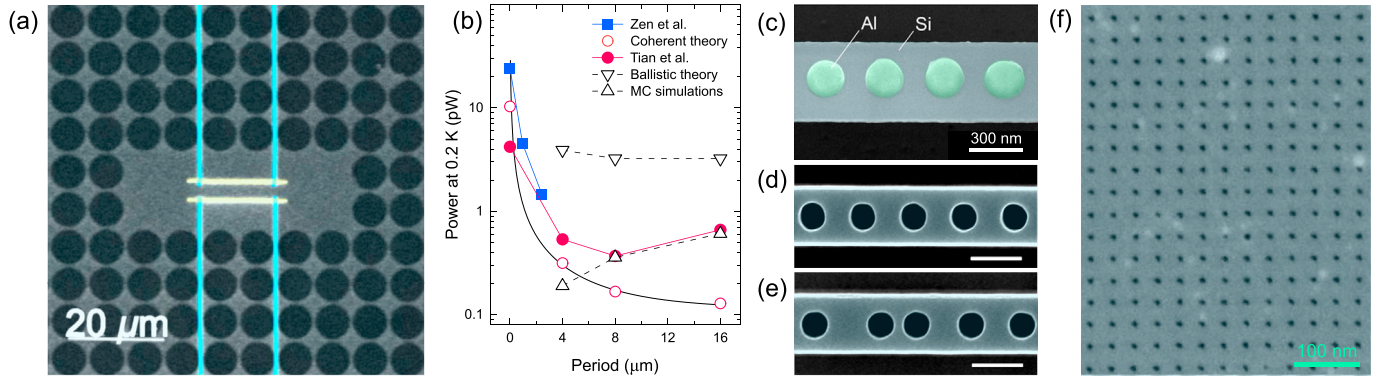

Fig. 8. PnCs and crossover of thermal conduction. (a) SEM image of a 2D hole-based PnC with a superconducting junction heater and sensor (yellow). (b) Measured power (squares [38] and filled circles [135]) and theoretical predictions of different models from Ref. [135]. The temperature was fixed at 0.2 K. A period of 0 corresponds to an unpatterned membrane. The lines are intended to guide the eyes. (c) SEM image of a one-dimensional pillar-based PnC [189]. (d–e) Ordered and disordered one-dimensional hole-based PnCs used to highlight coherent effects below 10 K [39]. (f) Two-dimensional hole-based PnC in suspended graphene with hole diameters of 7.6 nm [190]. Scale bars are 300 nm (c–e) and 100 nm (f). Adapted with permission from (a,b) [135], (c) [189], (d,e) [39], and (f) [190].

from incoherent surface scattering, although a decrease in the group velocity of phonons has also been proposed [198]. The use of pillars on membranes or periodic wings on nanobeams is a natural evolution of the periodic modulation of the width. It is equivalent from a conceptual point of view and introduces local resonances to the dispersion relation already modified due to the periodicity. Indeed, increasing the pillar size causes a stronger modification of the dispersion relation due to periodicity [194]; it also results in a larger number of local resonances [172], which together reduce the thermal conductivity. Theoretical studies predict that this effect would be enhanced with the addition of periodic wings on several sides of a nanobeam [181,199], but there is no experimental demonstration of this effect to date in the coherent thermal transport regime, despite several experimental attempts. An example of this is shown in Fig. 8(c) for a nanobeam topped by aluminum nanopillars; the modified thermal properties measured in pillar-based structures from room temperature to cryogenic temperatures can be explained by incoherent phonon scattering [189,200]. Although lower-frequency coherent acoustic modes have been experimentally demonstrated in such structures with the help of Brillouin light scattering [201] and asynchronous optical sampling at more than 50 GHz [202], the effect of coherence on the thermal conductivity remains to be proven experimentally. Recent reviews on this specific type of structure explain the findings in greater detail [8,15].

3.2.3. Superlattices and crossover of thermal conductivity

As discussed before, coherent control of thermal transport requires the interface roughness to be lower than the wavelength of phonons and dimensions over which the coherence is preserved. Superlattices are the most likely candidates to date to fit these prerequisites. Indeed, as multi-layer systems with alternating compositions, superlattices are essentially one-dimensional PnCs satisfying both conditions owing to fine control over layer thickness and have atomically flat interfaces. The literature on the thermal properties of superlattices is extensive, with both theoretical and experimental studies using many materials. One of the key experimental achievements is the demonstration of thermal conductivity below the amorphous limit [203–205]. In such structures, both diffuse phonon scattering due to the high density of interfaces and coherent thermal transport affect thermal conductivity, which remains lower than that of bulk materials. When the periods are long, the phonons do not experience periodicity and are mainly scattered diffusely at the interfaces. The thermal conductivity further decreases with period until coherence is achieved when the period is sufficiently small. This typically occurs for periods of a few nanometers, below which the trend is reversed. This phenomenon, that is, the crossover of thermal conductivity, is explained in greater detail in the previous sections. It was demonstrated experimentally for the first time by Ravichandran et al. [122] in oxide superlattices for a period of 2 nm. This crossover period increases as the temperature decreases owing to the increasing phonon wavelength. Other studies have reproduced the experiment with different superlattices [206,207] and made similar observations, although the temperature dependence of the crossover point has not been clearly highlighted. Superlattices provide an ideal experimental platform to study phonon localization, particularly Anderson localization. This phenomenon was observed at ~ 200 GHz in aperiodic superlattices [208] and affects the thermal conduction [10,152]. Sections 3.1.2 and 3.1.3 provide further information about this mechanism, which is also explained in a previous review of 1D structures [15]. To facilitate further experimentation and realize the design of optimized structures, a recent study has coupled phonon transport calculations and machine learning to suppress coherent thermal conduction, experimentally demonstrating lower thermal conductivity than the similar but periodic structures [24].

3.2.4. Novel materials and designs for PnCs

Coherent control of thermal transport is critical for developing the potential applications of PnCs, including thermal circuits, and standard operation cannot necessarily support lower temperatures. The first proposed strategy to circumvent this issue involves the use of a multiscale structure to filter the phonon spectrum so that heat is carried by phonons at lower frequencies and in a narrower range [209]. The other strategy to avoid low-temperature operation relies on lower dimensions. Self-assembling block copolymers have been used to demonstrate PnCs with short periods. However, improvement in surface roughness remains limited, and no coherent thermal transport has been measured to date. Using novel layered materials such as graphene enables further reduction of the dimensions, both in thickness and in the patterning dimension, as shown by Celebi et al. [190]. Regularly spaced holes smaller than 10 nm in diameter were fabricated using helium-focused ion beam drilling, as shown in Fig. 8(f). Similarly, carbon nanotubes have been used to fabricate structures with similarly small dimensions [210], which modify the thermal properties. Such dimensions in materials known for the extremely long MFPs of their phonons promise higher working temperatures for coherent thermal control. This approach toward materials with long phonon MFPs is now being investigated [102] for applications in thermal management, particularly in materials with ultrahigh thermal conductivity rivaling that of diamond [211–215]. With the large existing body of literature and the ever more complex PnCs designs, manual investigation becomes limited. Preexisting results can thus be used for data driven investigation, with machine learning. This method has already been largely used for PnCs [127,165–167,169,216–218] and even combined with experiments to demonstrate an aperiodic superlattice with a lower thermal conductivity than that of the periodic one [24]. Machine learning based designs and materials are still a growing area with improvements expected in more complex designs such as 3D PnCs, as well as combining fabrication capabilities with some of the novel materials mentioned above. Some optimization directions include the creation of larger or more robust bandgaps, the minimization of the thermal conductivity, the increase in hybridization tuning of specific interface properties to cite a few. Beyond PnCs, it is also interesting to note that the interface between PnCs and pristine materials can be used as a thermal interface with controllable properties such as an increased thermal interface conductance when compared to two dissimilar materials with identical weight ratio or thermal conductivity ratio [219]. Whereas this type of interface can suppress thermal rectification, some asymmetric structures have been proposed to rectify the heat flux in specific conditions, with existing experimental demonstration in graphene [220].

4. Conclusions and prospects

This review presented a panorama of recent advancements in the manipulation of heat via PnCs. Incoherent thermal transport involves altering the properties of the gas of phonon particles through scattering with well-designed surfaces, for example, circular holes in a membrane. In this frame, predictions provide satisfactory agreement with measurements except in the case of very small necks, where the heat flux has lower values than those provided by the phonon gas model. The source of this disagreement has been investigated, and a possible answer might be found in the

alteration of mechanical properties in sub-50-nm structures. Coherent thermal transport has excited the utmost curiosity of physicists investigating the fundamental behaviors in the hope of highlighting the wave nature of the phonon particle itself. Several experimental attempts have concluded the existence of this coherence, whereas later studies have attenuated these outcomes. However, investigations performed in periods of 100 nm at sub-ten kelvin or in the nanometer scale at room temperature appear more convincing. Theoretical studies extending to extremely small structures and low temperatures were also able to unfold the rich scope of new wave-related phenomena. The effect of PnCs on the wave features of heat differs from that observed in the acoustic field as well as in photonic crystals. Indeed, the density and elevated frequencies of thermal phonon modes make the creation of gaps at low frequencies ineffective. Nanostructurization mostly affects the group velocity, and eventually, the MFP. In the case of disordered structures and elastic scattering, backscattering resulting in weak to strong localization in 2D materials was also predicted through simulation. Although these latter effects require ultra-low temperatures and perfect control of the surface state, 2D materials appear to be ideal candidates to uncover a large variety of wave effects in phonon heat transport.

Data availability

Data is available from the corresponding author on request.

Funding

This work was supported by CREST JST [grant number JPMJCR19Q3]; PRESTO JST [grant number JPMJPR19I1]; KAKENHI and Postdoctoral Fellowship of the Japan Society for the Promotion of Science [grant numbers 21H04635 and P19353]; and the European Union's Horizon 2020 Research and Innovation Programme under the Marie Skłodowska-Curie Individual Fellowship NATELM [grant number 898 079].

Declaration of competing interest

The authors declare that they have no known competing financial interests or personal relationships that could have appeared to influence the work reported in this paper.

References

[1] M. Eichenfield, J. Chan, R.M. Camacho, K.J. Vahala, O. Painter, Optomechanical crystals, Nature 462 (7269) (2009) 78–82.
[2] D. Hatanaka, I. Mahboob, K. Onomitsu, H. Yamaguchi, Phonon waveguides for electromechanical circuits, Nat. Nanotechnol. 9 (7) (2014) 520–524.
[3] P.A. Deymier, Acoustic Metamaterials and Phononic Crystals, vol. 173, Springer Science & Business Media, 2013.
[4] Y. Pennec, B. Djafari-Rouhani, Fundamental properties of phononic crystal, in: Phononic Crystals, Springer, 2016, pp. 23–50.
[5] J. Liu, H. Guo, T. Wang, A review of acoustic metamaterials and phononic crystals, Crystals 10 (4) (2020) 305.
[6] M. Sledzinska, B. Graczykowski, J. Maire, E. Chavez-Angel, C.M. Sotomayor-Torres, F. Alzina, 2D phononic crystals: progress and prospects in hypersound and thermal transport engineering, Adv. Funct. Mater. 30 (8) (2020) 1904434, https://doi.org/10.1002/adfm.201904434.
[7] T. Vasileiadis, J. Varghese, V. Babacic, J. Gomis-Bresco, D. Navarro Urrios, B. Graczykowski, Progress and perspectives on phononic crystals, J. Appl. Phys. 129 (16) (2021) 160901.
[8] Y. Jin, Y. Pennec, B. Bonello, H. Honarvar, L. Dobrzynski, B. Djafari-Rouhani, M. I. Hussein, reportPhysics of Surface Vibrational Resonances: Pillared Phononic Crystals, Metamaterials, and Metasurfaces, Reports on Progress in Physicsdoi:10.1088/1361-6633/abdab8.
[9] R. Anufriev, M. Nomura, Ray phononics: thermal guides, emitters, filters, and shields powered by ballistic phonon transport, Mater. Today Phy. 15 (2020) 100272.
[10] Y. Guo, M. Bescond, Z. Zhang, S. Xiong, K. Hirakawa, M. Nomura, S. Volz, Thermal conductivity minimum of graded superlattices due to phonon localization, Apl. Mater. 9 (April) (2021): 091104, https://doi.org/10.1063/5.0054921.
[11] K. Esfarjani, G. Chen, H.T. Stokes, Heat transport in silicon from first-principles calculations, Phys. Rev. B 84 (8) (2011): 085204.
[12] N. Uchida, T. Tada, Y. Ohishi, Y. Miyazaki, K. Kurosaki, S. Yamanaka, Heavily doped silicon and nickel silicide nanocrystal composite films with enhanced thermoelectric efficiency, J. Appl. Phys. 114 (13) (2013) 134311.
[13] S. Yamasaka, Y. Nakamura, T. Ueda, S. Takeuchi, A. Sakai, Phonon transport control by nanoarchitecture including epitaxial ge nanodots for si-based thermoelectric materials, Sci. Rep. 5 (1) (2015) 1–9.
[14] A.I. Hochbaum, R. Chen, R.D. Delgado, W. Liang, E.C. Garnett, M. Najarian, A. Majumdar, P. Yang, Enhanced thermoelectric performance of rough silicon nanowires, Nature 451 (7175) (2008) 163–167.
[15] R. Anufriev, J. Maire, M. Nomura, Review of coherent phonon and heat transport control in one-dimensional phononic crystals at nanoscale, Apl. Mater. 9 (7) (2021): 070701, https://doi.org/10.1063/5.0052230.
[16] M. Asheghi, Y. Leung, S. Wong, K. Goodson, Phonon-boundary scattering in thin silicon layers, Appl. Phys. Lett. 71 (13) (1997) 1798–1800.
[17] E. Chávez-Ángel, J.S. Reparaz, J. Gomis-Bresco, M.R. Wagner, J. Cuffe, B. Graczykowski, A. Shchepetov, H. Jiang, M. Prunnila, J. Ahopelto, et al., Reduction of the thermal conductivity in free-standing silicon nano-membranes investigated by non-invasive Raman thermometry, Apl. Mater. 2 (1) (2014): 012113.
[18] B.L. Davis, M.I. Hussein, Nanophononic metamaterial: thermal conductivity reduction by local resonance, Phys. Rev. Lett. 112 (5) (2014): 055505, https://doi.org/10.1103/PhysRevLett.112.055505.
[19] R. Anufriev, M. Nomura, Phonon and heat transport control using pillar-based phononic crystals, Sci. Technol. Adv. Mater. 19 (1) (2018) 863–870, https://doi.org/10.1080/14686996.2018.1542524.
[20] D. Song, G. Chen, Thermal conductivity of periodic microporous silicon films, Appl. Phys. Lett. 84 (5) (2004) 687–689.
[21] J. Tang, H.-T. Wang, D.H. Lee, M. Fardy, Z. Huo, T.P. Russell, P. Yang, Holey silicon as an efficient thermoelectric material, Nano Lett. 10 (10) (2010) 4279–4283, https://doi.org/10.1021/nl102931z.
[22] J. Lim, H.-T.T. Wang, J. Tang, S.C. Andrews, H. So, J. Lee, D.H. Lee, T.P. Russell, P. Yang, Simultaneous thermoelectric property measurement and incoherent phonon transport in holey silicon, ACS Nano 10 (1) (2016) 124–132, https://doi.org/10.1021/acsnano.5b05385.
[23] Y. Xiao, D. Xu, F.J. Medina, S. Wang, Q. Hao, Thermal studies of nanoporous thin films with added periodic nanopores—a new approach to evaluate the importance of phononic effects, Mater. Today Phy. 12 (2020) 100179.
[24] R. Hu, S. Iwamoto, L. Feng, S. Ju, S. Hu, M. Ohnishi, N. Nagai, K. Hirakawa, J. Shiomi, Machine-learning-optimized aperiodic superlattice minimizes coherent phonon heat conduction, Phys. Rev. X 10 (2) (2020): 021050, https://doi.org/10.1103/PhysRevX.10.021050.
[25] J.-K. Yu, S. Mitrovic, D. Tham, J. Varghese, J.R. Heath, Reduction of thermal conductivity in phononic nanomesh structures, Nat. Nanotechnol. 5 (10) (2010) 718–721, https://doi.org/10.1038/nnano.2010.149.
[26] P.E. Hopkins, L.M. Phinney, P.T. Rakich, R.H. Olsson, I. El-Kady, Phonon considerations in the reduction of thermal conductivity in phononic crystals, Appl. Phys. Mater. Sci. Process 103 (3) (2011) 575–579, https://doi.org/10.1007/s00339-010-6189-8.
[27] I. El-Kady, R. H. Olsson III, P. E. Hopkins, Z. C. Leseman, D. F. Goettler, B. Kim, C. M. Reinke, M. F. Su, reportPhonon Manipulation with Phononic Crystals, Sandia National Labs, Albuquerque, NM, Report No. SAND2012-0127.
[28] M. Nomura, J. Nakagawa, Y. Kage, J. Maire, D. Moser, O. Paul, Thermal phonon transport in silicon nanowires and two-dimensional phononic crystal nanostructures, Appl. Phys. Lett. 106 (14) (2015) 143102.
[29] D.G. Cahill, K. Goodson, A. Majumdar, Thermometry and thermal transport in micro/nanoscale solid-state devices and structures, J. Heat Tran. 124 (2) (2002) 223–241.
[30] T. Luo, G. Chen, Nanoscale heat transfer–from computation to experiment, Phys. Chem. Chem. Phys. 15 (10) (2013) 3389–3412.
[31] D.G. Cahill, P.V. Braun, G. Chen, D.R. Clarke, S. Fan, K.E. Goodson, P. Keblinski, W.P. King, G.D. Mahan, A. Majumdar, et al., Nanoscale thermal transport. ii, Appl. Phys. Rev. 1 (1) (2014): 011305, 2003–2012.
[32] S. Volz, J. Ordonez-Miranda, A. Shchepetov, M. Prunnila, J. Ahopelto, T. Pezeril, G. Vaudel, V. Gusev, P. Ruello, E.M. Weig, et al., Nanophononics: state of the art and perspectives, Euro. Phys. J. 89 (1) (2016) 1–20.
[33] M. Nomura, J. Shiomi, T. Shiga, R. Anufriev, Thermal phonon engineering by tailored nanostructures, Jpn. J. Appl. Phys. 57 (8) (2018): 080101, https://doi.org/10.7567/jjap.57.080101.
[34] Y. Li, W. Li, T. Han, X. Zheng, J. Li, B. Li, S. Fan, C.-W. Qiu, Transforming heat transfer with thermal metamaterials and devices, Nat. Rev. Mater. 6 (6) (2021) 488–507.
[35] R. Anufriev, A. Ramiere, J. Maire, M. Nomura, Heat guiding and focusing using ballistic phonon transport in phononic nanostructures, Nat. Commun. 8 (1) (2017) 1–8.
[36] E. Dechaumphai, R. Chen, Thermal transport in phononic crystals: the role of zone folding effect, J. Appl. Phys. 111 (7) (2012): 073508, https://doi.org/10.1063/1.3699056.
[37] Narayanamurti, Selective transmission of high-frequency phonons by a superlattice, Phys. Rev. Lett. 43 (27) (1979) 2012.
[38] N. Zen, T.a. Puurtinen, T.J. Isotalo, S. Chaudhuri, I.J. Maasilta, Engineering thermal conductance using a two-dimensional phononic crystal, Nat.

Commun. 5 (1) (2014) 3435, https://doi.org/10.1038/ncomms4435.
[39] J. Maire, R. Anufriev, R. Yanagisawa, A. Ramiere, S. Volz, M. Nomura, Heat conduction tuning by wave nature of phonons, Sci. Adv. 3 (8) (2017): e1700027, https://doi.org/10.1126/sciadv.1700027 arXiv:arXiv:1508.04574.
[40] S. Yang, J.H. Page, Z. Liu, M.L. Cowan, C.T. Chan, P. Sheng, Ultrasound tunneling through 3d phononic crystals, Phys. Rev. Lett. 88 (10) (2002) 104301.
[41] S. Yang, J. Page, Z. Liu, M. Cowan, C. Chan, P. Sheng, Focusing of sound in a 3D phononic crystal, Phys. Rev. Lett. 93 (2) (2004): 024301, https://doi.org/10.1103/PhysRevLett.93.024301.
[42] L. D'Alessandro, E. Belloni, R. Ardito, A. Corigliano, F. Braghin, Modeling and experimental verification of an ultra-wide bandgap in 3d phononic crystal, Appl. Phys. Lett. 109 (22) (2016) 221907.
[43] L. Yang, N. Yang, B. Li, Reduction of thermal conductivity by nanoscale 3d phononic crystal, Sci. Rep. 3 (1) (2013) 1–5.
[44] L. Yang, N. Yang, B. Li, Extreme low thermal conductivity in nanoscale 3d si phononic crystal with spherical pores, Nano Lett. 14 (4) (2014) 1734–1738.
[45] R.E. Peierls, Quantum Theory of Solids, Clarendon Press, Oxford, 1955.
[46] J.M. Ziman, Electrons and Phonons: the Theory of Transport Phenomena in Solids, Oxford University Press, New York, 2001.
[47] L. Lindsay, C. Hua, X. Ruan, S. Lee, Survey of ab initio phonon thermal transport, Mater. Today Phy. 7 (2018) 106–120, https://doi.org/10.1016/j.mtphys.2018.11.008. https://www.sciencedirect.com/science/article/pii/S254252931830141X.
[48] S.G. Volz, G. Chen, Molecular-dynamics simulation of thermal conductivity of silicon crystals, Phys. Rev. B 61 (4) (2000) 2651–2656, https://doi.org/10.1103/PhysRevB.61.2651.
[49] Y. Chen, D. Li, J.R. Lukes, Z. Ni, M. Chen, Minimum superlattice thermal conductivity from molecular dynamics, Phys. Rev. B 72 (17) (2005) 174302, https://doi.org/10.1103/PhysRevB.72.174302.
[50] N. Mingo, Anharmonic phonon flow through molecular-sized junctions, Phys. Rev. B 74 (12) (2006) 125402, https://doi.org/10.1103/PhysRevB.74.125402.
[51] Y. Guo, M. Bescond, Z. Zhang, M. Luisier, M. Nomura, S. Volz, Quantum mechanical modeling of anharmonic phonon-phonon scattering in nanostructures, Phys. Rev. B 102 (19) (2020) 195412, https://doi.org/10.1103/PhysRevB.102.195412.
[52] Q. Hao, Y. Xiao, H. Zhao, Analytical model for phonon transport analysis of periodic bulk nanoporous structures, Appl. Therm. Eng. 111 (2017) 1409–1416, https://doi.org/10.1016/j.applthermaleng.2016.06.075.
[53] G. Xie, Z. Ju, K. Zhou, X. Wei, Z. Guo, Y. Cai, G. Zhang, Ultra-low thermal conductivity of two-dimensional phononic crystals in the incoherent regime, Comput. Mater. 4 (1) (2018) 21, https://doi.org/10.1038/s41524-018-0076-9.
[54] A. Jain, Y.-J. Yu, A.J. McGaughey, Phonon transport in periodic silicon nanoporous films with feature sizes greater than 100 nm, Phys. Rev. B 87 (19) (2013) 195301, https://doi.org/10.1103/PhysRevB.87.195301.
[55] K.D. Parrish, J.R. Abel, A. Jain, J.A. Malen, A.J. McGaughey, Phonon-boundary scattering in nanoporous silicon films: comparison of Monte Carlo techniques, J. Appl. Phys. 122 (12) (2017) 125101, https://doi.org/10.1063/1.4993601.
[56] R. Yang, G. Chen, M.S. Dresselhaus, Thermal conductivity of simple and tubular nanowire composites in the longitudinal direction, Phys. Rev. B 72 (12) (2005) 125418, https://doi.org/10.1103/PhysRevB.72.125418.
[57] T.-Y. Hsieh, H. Lin, T.-J. Hsieh, J.-C. Huang, Thermal conductivity modeling of periodic porous silicon with aligned cylindrical pores, J. Appl. Phys. 111 (12) (2012) 124329, https://doi.org/10.1063/1.4730962.
[58] G. Tang, C. Bi, B. Fu, Thermal conduction in nano-porous silicon thin film, J. Appl. Phys. 114 (18) (2013) 184302, https://doi.org/10.1063/1.4829913.
[59] G. Romano, K. Esfarjani, D.A. Strubbe, D. Broido, A.M. Kolpak, Temperature-dependent thermal conductivity in silicon nanostructured materials studied by the Boltzmann transport equation, Phys. Rev. B 93 (3) (2016): 035408, https://doi.org/10.1103/PhysRevB.93.035408.
[60] Q. Hao, G. Chen, M.-S. Jeng, Frequency-dependent Monte Carlo simulations of phonon transport in two-dimensional porous silicon with aligned pores, J. Appl. Phys. 106 (11) (2009) 114321, https://doi.org/10.1063/1.3266169.
[61] S. Wolf, N. Neophytou, H. Kosina, Thermal conductivity of silicon nanomeshes: effects of porosity and roughness, J. Appl. Phys. 115 (20) (2014) 204306, https://doi.org/10.1063/1.4879242.
[62] V. Jean, S. Fumeron, K. Termentzidis, S. Tutashkonko, D. Lacroix, Monte Carlo simulations of phonon transport in nanoporous silicon and germanium, J. Appl. Phys. 115 (2) (2014): 024304, https://doi.org/10.1063/1.4861410.
[63] N.K. Ravichandran, A.J. Minnich, Coherent and incoherent thermal transport in nanomeshes, Phys. Rev. B 89 (20) (2014) 205432, https://doi.org/10.1103/PhysRevB.89.205432.
[64] J.-P.M. Péraud, N.G. Hadjiconstantinou, Efficient simulation of multidimensional phonon transport using energy-based variance-reduced Monte Carlo formulations, Phys. Rev. B 84 (20) (2011) 205331, https://doi.org/10.1103/PhysRevB.84.205331.
[65] J.-P. M. Péraud, C. D. Landon, N. G. Hadjiconstantinou, Monte Carlo methods for solving the Boltzmann transport equation, Ann. Rev. Heat Trans. 17. doi: 10.1615/AnnualRevHeatTransfer.2014007381.
[66] G. Chen, Thermal conductivity and ballistic-phonon transport in the cross-plane direction of superlattices, Phys. Rev. B 57 (23) (1998) 14958, https://doi.org/10.1103/PhysRevB.57.14958.
[67] B. Latour, S. Volz, Y. Chalopin, Microscopic description of thermal-phonon coherence: from coherent transport to diffuse interface scattering in superlattices, Phys. Rev. B 90 (1) (2014): 014307, https://doi.org/10.1103/PhysRevB.90.014307.
[68] K. Kothari, M. Maldovan, Phonon surface scattering and thermal energy distribution in superlattices, Sci. Rep. 7 (1) (2017) 1–15, https://doi.org/10.1038/s41598-017-05631-3.
[69] E. Ye, A.J. Minnich, Ab initio based investigation of thermal transport in superlattices using the Boltzmann equation: assessing the role of phonon coherence, J. Appl. Phys. 125 (5) (2019): 055107, https://doi.org/10.1063/1.5075481.
[70] X. Ran, M. Wang, In-plane interfacial phonon transport through multi-layer thin films by theoretical analyses and Monte Carlo simulations, Int. J. Heat Mass Tran. 176 (2021) 121438, https://doi.org/10.1016/j.ijheatmasstransfer.2021.121438.
[71] Y. Guo, M. Wang, Phonon hydrodynamics and its applications in nanoscale heat transport, Phys. Rep. 595 (2015) 1–44, https://doi.org/10.1016/j.physrep.2015.07.003.
[72] S. Lee, D. Broido, K. Esfarjani, G. Chen, Hydrodynamic phonon transport in suspended graphene, Nat. Commun. 6 (1) (2015) 1–10, https://doi.org/10.1038/ncomms7290.
[73] A. Cepellotti, G. Fugallo, L. Paulatto, M. Lazzeri, F. Mauri, N. Marzari, Phonon hydrodynamics in two-dimensional materials, Nat. Commun. 6 (1) (2015) 1–7, https://doi.org/10.1038/ncomms7400.
[74] Y. Guo, M. Wang, Heat transport in two-dimensional materials by directly solving the phonon Boltzmann equation under callaway's dual relaxation model, Phys. Rev. B 96 (13) (2017) 134312, https://doi.org/10.1103/PhysRevB.96.134312.
[75] Y. Guo, Z. Zhang, M. Nomura, S. Volz, M. Wang, Phonon vortex dynamics in graphene ribbon by solving Boltzmann transport equation with ab initio scattering rates, Int. J. Heat Mass Tran. 169 (2021) 120981, https://doi.org/10.1016/j.ijheatmasstransfer.2021.120981.
[76] K.T. Regner, J.P. Freedman, J.A. Malen, Advances in studying phonon mean-free-path-dependent contributions to thermal conductivity, Nanoscale Microscale Thermophys. Eng. 19 (2015) 183–205, https://doi.org/10.1080/15567265.2015.1045640.
[77] R. Anufriev, J. Ordonez-Miranda, M. Nomura, Measurement of the phonon mean free path spectrum in silicon membranes at different temperatures using arrays of nanoslits, Phys. Rev. B 101 (2020) 115301.
[78] A. Malhotra, M. Maldovan, Surface scattering controlled heat conduction in semiconductor thin films, J. Appl. Phys. 120 (20) (2016) 204305, https://doi.org/10.1063/1.4968542.
[79] M. Nomura, Y. Kage, J. Nakagawa, T. Hori, J. Maire, J. Shiomi, R. Anufriev, D. Moser, O. Paul, Impeded thermal transport in si multiscale hierarchical architectures with phononic crystal nanostructures, Phys. Rev. B 91 (2015) 205422, https://doi.org/10.1103/PhysRevB.91.205422. https://link.aps.org/doi/10.1103/PhysRevB.91.205422.
[80] A. Eucken, Allgemeine Gesetzmäßigkeiten für das Wärmeleitvermögen verschiedener Stoffarten und Aggregatzustände, Ausgabe A 11 (1) (1940) 6–20, https://doi.org/10.1007/BF02584103.
[81] R. Anufriev, A. Ramiere, J. Maire, M. Nomura, Heat guiding and focusing using ballistic phonon transport in phononic nanostructures, Nat. Commun. 8 (May) (2017) 15505, https://doi.org/10.1038/ncomms15505.
[82] K. Takahashi, M. Fujikane, Y. Liao, M. Kashiwagi, T. Kawasaki, N. Tambo, S. Ju, Y. Naito, J. Shiomi, Elastic inhomogeneity and anomalous thermal transport in ultrafine si phononic crystals, Nano Energy 71 (2020) 104581.
[83] R. Anufriev, J. Maire, M. Nomura, Reduction of thermal conductivity by surface scattering of phonons in periodic silicon nanostructures, Phys. Rev. B 93 (2016): 045411.
[84] J. Nakagawa, Y. Kage, T. Hori, J. Shiomi, M. Nomura, Crystal structure dependent thermal conductivity in two-dimensional phononic crystal nanostructures, Appl. Phys. Lett. 107 (2) (2015): 023104, https://doi.org/10.1063/1.4926653.
[85] B. Kim, J. Nguyen, C. Reinke, E. Shaner, C.T. Harris, I. El-kady, R.H.O. Iii, Thermal conductivity manipulation in lithographically patterned single crystal silicon phononic crystal structures, in: International Ultrasonics Symposium Proceedings, 2011, pp. 1308–1311.
[86] Q. Hao, D. Xu, H. Zhao, Y. Xiao, F.J. Medina, Thermal studies of nanoporous Si films with pitches on the order of 100 nm-comparison between different pore-drilling techniques, Sci. Rep. 8 (1) (2018) 9056, https://doi.org/10.1038/s41598-018-26872-w.
[87] M.R. Wagner, B. Graczykowski, J.S. Reparaz, A. El Sachat, M. Sledzinska, F. Alzina, C.M. Sotomayor Torres, Two-dimensional phononic crystals: disorder matters, Nano Lett. 16 (2016) 5661–5668, https://doi.org/10.1021/acs.nanolett.6b02305, arXiv:1511.07398.
[88] L. Maurer, Z. Aksamija, E. Ramayya, A. Davoody, I. Knezevic, Universal features of phonon transport in nanowires with correlated surface roughness, Appl. Phys. Lett. 106 (13) (2015) 133108.
[89] J. Lim, K. Hippalgaonkar, S. Andrews, A. Majumdar, P. Yang, Quantifying surface roughness effects on phonon transport in silicon nanowires, Nano Lett. 12 (5) (2012) 2475–2482, https://doi.org/10.1021/nl3005868.
[90] R. Yanagisawa, J. Maire, A. Ramiere, R. Anufriev, M. Nomura, Impact of limiting dimension on thermal conductivity of one-dimensional silicon phononic crystals, Appl. Phys. Lett. 110 (13) (2017) 133108, https://doi.org/10.1063/1.4979080.
[91] M. Verdier, R. Anufriev, A. Ramiere, K. Termentzidis, D. Lacroix, Thermal

conductivity of phononic membranes with aligned and staggered lattices of holes at room and low temperatures, Phys. Rev. B 95 (20) (2017) 205438, https://doi.org/10.1103/PhysRevB.95.205438.
[92] M. Verdier, K. Termentzidis, D. Lacroix, Crystalline-amorphous silicon nanocomposites: nano-pores and nano-inclusions impact on the thermal conductivity, J. Appl. Phys. 119 (17) (2016) 175104, https://doi.org/10.1063/1.4948337.
[93] B. Graczykowski, A. El Sachat, J.S. Reparaz, M. Sledzinska, M.R. Wagner, E. Chavez-Angel, Y. Wu, S. Volz, Y. Wu, F. Alzina, C.M. Sotomayor Torres, Thermal conductivity and air-mediated losses in periodic porous silicon membranes at high temperatures, Nat. Commun. 8 (1) (2017) 415, https://doi.org/10.1038/s41467-017-00115-4.
[94] G.J. Snyder, E.S. Toberer, Complex Thermoelectric Materials, Materials for Sustainable Energy: a Collection of Peer-Reviewed Research and Review Articles from, Nature Publishing Group, 2011, pp. 101–110.
[95] K. Kōmoto, T. Mori, Thermoelectric Nanomaterials: Materials Design and Applications, Springer, 2013.
[96] X.-L. Shi, J. Zou, Z.-G. Chen, Advanced thermoelectric design: from materials and structures to devices, Chem. Rev. 120 (15) (2020) 7399–7515.
[97] Z. Soleimani, S. Zoras, B. Ceranic, S. Shahzad, Y. Cui, A review on recent developments of thermoelectric materials for room-temperature applications, Sustain. Energy Technol. Assessments 37 (2020) 100604.
[98] Y. Pei, X. Shi, A. LaLonde, H. Wang, L. Chen, G.J. Snyder, Convergence of electronic bands for high performance bulk thermoelectrics, Nature 473 (7345) (2011) 66–69.
[99] C. Fu, S. Bai, Y. Liu, Y. Tang, L. Chen, X. Zhao, T. Zhu, Realizing high figure of merit in heavy-band p-type half-heusler thermoelectric materials, Nat. Commun. 6 (1) (2015) 1–7.
[100] B. Hinterleitner, I. Knapp, M. Poneder, Y. Shi, H. Müller, G. Eguchi, C. Eisenmenger-Sittner, M. Stöger-Pollach, Y. Kakefuda, N. Kawamoto, et al., Thermoelectric performance of a metastable thin-film heusler alloy, Nature 576 (7785) (2019) 85–90.
[101] G.A. Slack, New Materials and Performance Limits for Thermoelectric Cooling, CRC handbook of thermoelectrics, 1995, pp. 407–440.
[102] J.P. Freedman, J.H. Leach, E.A. Preble, Z. Sitar, R.F. Davis, J.A. Malen, Universal phonon mean free path spectra in crystalline semiconductors at high temperature, Sci. Rep. 3 (1) (2013) 2963, https://doi.org/10.1038/srep02963.
[103] Y. Hu, L. Zeng, A.J. Minnich, M.S. Dresselhaus, G. Chen, Spectral mapping of thermal conductivity through nanoscale ballistic transport, Nat. Nanotechnol. 10 (8) (2015) 701–706.
[104] J.S. Kang, M. Li, H. Wu, H. Nguyen, Y. Hu, Experimental observation of high thermal conductivity in boron arsenide, Science 361 (6402) (2018) 575–578.
[105] J. Verwey, R. Kramer, B. De Maagt, Mean free path of hot electrons at the surface of boron-doped silicon, J. Appl. Phys. 46 (6) (1975) 2612–2619.
[106] A.I. Boukai, Y. Bunimovich, J. Tahir-Kheli, J.-K. Yu, W.A. Goddard Iii, J.R. Heath, Silicon nanowires as efficient thermoelectric materials, nature 451 (7175) (2008) 168–171.
[107] P.E. Hopkins, C.M. Reinke, M.F. Su, R.H. Olsson III, E.A. Shaner, Z.C. Leseman, J.R. Serrano, L.M. Phinney, I. El-Kady, Reduction in the thermal conductivity of single crystalline silicon by phononic crystal patterning, Nano Lett. 11 (1) (2011) 107–112.
[108] M. Nomura, Y. Kage, D. Müller, D. Moser, O. Paul, Electrical and thermal properties of polycrystalline Si thin films with phononic crystal nanopatterning for thermoelectric applications, Appl. Phys. Lett. 106 (22) (2015) 223106, https://doi.org/10.1063/1.4922198.
[109] J. Shiomi, Research update: phonon engineering of nanocrystalline silicon thermoelectrics, Apl. Mater. 4 (10) (2016) 104504.
[110] X. Huang, S. Gluchko, R. Anufriev, S. Volz, M. Nomura, Thermal conductivity reduction in a silicon thin film with nanocones, ACS Appl. Mater. Interfaces 11 (37) (2019) 34394–34398.
[111] A. George, R. Yanagisawa, R. Anufriev, J. He, N. Yoshie, N. Tsujii, Q. Guo, T. Mori, S. Volz, M. Nomura, Thermoelectric enhancement of silicon membranes by ultrathin amorphous films, ACS Appl. Mater. Interfaces 11 (12) (2019) 12027–12031.
[112] N. Liu, T. Zhu, M.G. Rosul, J. Peters, J.E. Bowers, M. Zebarjadi, Thermoelectric properties of holey silicon at elevated temperatures, Mater. Today Phy. 14 (2020) 100224.
[113] M. Strasser, R. Aigner, M. Franosch, G. Wachutka, Miniaturized thermoelectric generators based on poly-si and poly-sige surface micromachining, Sensor Actuator Phys. 97 (2002) 535–542.
[114] P.-H. Kao, P.-J. Shih, C.-L. Dai, M.-C. Liu, Fabrication and characterization of cmos-mems thermoelectric micro generators, Sensors 10 (2) (2010) 1315–1325.
[115] J. Xie, C. Lee, H. Feng, Design, fabrication, and characterization of cmos mems-based thermoelectric power generators, J. Microelectr. Syst. 19 (2) (2010) 317–324.
[116] T. Zhan, R. Yamato, S. Hashimoto, M. Tomita, S. Oba, Y. Himeda, K. Mesaki, H. Takezawa, R. Yokogawa, Y. Xu, et al., Miniaturized planar si-nanowire micro-thermoelectric generator using exuded thermal field for power generation, Sci. Technol. Adv. Mater. 19 (1) (2018) 443–453.
[117] G. Hu, H. Edwards, M. Lee, Silicon integrated circuit thermoelectric generators with a high specific power generation capacity, Nat. Electr. 2 (7) (2019) 300–306.
[118] R. Yanagisawa, N. Tsujii, T. Mori, P. Ruther, O. Paul, M. Nomura, Nanostructured planar-type uni-leg si thermoelectric generators, APEX 13 (9) (2020): 095001.
[119] S. Yang, S. Wang, Development of a thermoelectric energy generator with double cavity by standard cmos process, IEEE Sensor. J. 21 (1) (2020) 250–256.
[120] J. Garg, G. Chen, Minimum thermal conductivity in superlattices: a first-principles formalism, Phys. Rev. B 87 (14) (2013) 140302, https://doi.org/10.1103/PhysRevB.87.140302.
[121] X.K. Chen, Z.X. Xie, W.X. Zhou, L.M. Tang, K.Q. Chen, Phonon wave interference in graphene and boron nitride superlattice, Appl. Phys. Lett. 109 (2) (2016) 107–112, https://doi.org/10.1063/1.4958688.
[122] J. Ravichandran, A.K. Yadav, R. Cheaito, P.B. Rossen, A. Soukiassian, S.J. Suresha, J.C. Duda, B.M. Foley, C.-H. Lee, Y. Zhu, A.W. Lichtenberger, J.E. Moore, D.A. Muller, D.G. Schlom, P.E. Hopkins, A. Majumdar, R. Ramesh, M.A. Zurbuchen, Crossover from incoherent to coherent phonon scattering in epitaxial oxide superlattices, Nat. Mater. 13 (2) (2014) 168–172, https://doi.org/10.1038/nmat3826.
[123] T. Zhu, E. Ertekin, Phonon transport on two-dimensional graphene/boron nitride superlattices, Phys. Rev. B 90 (19) (2014) 195209, https://doi.org/10.1103/PhysRevB.90.195209.
[124] G. Xie, D. Ding, G. Zhang, Phonon coherence and its effect on thermal conductivity of nanostructures, Adv. Phys. X 3 (1) (2018) 720–755, https://doi.org/10.1080/23746149.2018.1480417.
[125] B. Latour, Y. Chalopin, Distinguishing between spatial coherence and temporal coherence of phonons, Phys. Rev. B 95 (21) (2017) 214310, https://doi.org/10.1103/PhysRevB.95.214310.
[126] Z. Zhang, Y. Ouyang, Y. Cheng, J. Chen, N. Li, G. Zhang, Size-dependent phononic thermal transport in low-dimensional nanomaterials, Phys. Rep. 860 (2020) 1–26, https://doi.org/10.1016/j.physrep.2020.03.001.
[127] Z. Zhang, Y. Guo, M. Bescond, J. Chen, M. Nomura, S. Volz, Coherent thermal transport in nano-phononic crystals: an overview, Apl. Mater. 9 (8) (2021) 81102.
[128] Z. Zhang, Y. Guo, M. Bescond, J. Chen, M. Nomura, S. Volz, Thermal self-synchronization of nano-objects, J. Appl. Phys. 130 (8) (2021) 84301, https://doi.org/10.1063/5.0058252.
[129] G.P. Srivastava, The Physics of Phonons, Routledge, 2019.
[130] M.V. Simkin, G.D. Mahan, Minimum thermal conductivity of superlattices, Phys. Rev. Lett. 84 (5) (2000) 927–930, https://doi.org/10.1103/PhysRevLett.84.927.
[131] T. Juntunen, O. Vänskä, I. Tittonen, Anderson localization quenches thermal transport in aperiodic superlattices, Phys. Rev. Lett. 122 (10) (2019) 105901, https://doi.org/10.1103/PhysRevLett.122.105901.
[132] J. Garg, N. Bonini, N. Marzari, High thermal conductivity in short-period superlattices, Nano Lett. 11 (12) (2011) 5135–5141, https://doi.org/10.1021/nl202186y.
[133] S.C. Huberman, J.M. Larkin, A.J. McGaughey, C.H. Amon, Disruption of superlattice phonons by interfacial mixing, Phys. Rev. B 88 (15) (2013) 155311, https://doi.org/10.1103/PhysRevB.88.155311.
[134] T.A. Puurtinen, I.J. Maasilta, Low-Temperature coherent thermal conduction in thin phononic crystal membranes, Crystals 6 (6) (2016) 72, https://doi.org/10.3390/cryst6060072.
[135] Y. Tian, T.A. Puurtinen, Z. Geng, I.J. Maasilta, Minimizing coherent thermal conductance by controlling the periodicity of two-dimensional phononic crystals, Phy. Rev. Appl. 12 (1) (2019): 014008, https://doi.org/10.1103/PhysRevApplied.12.014008.
[136] W.S. Capinski, H.J. Maris, T. Ruf, M. Cardona, K. Ploog, D.S. Katzer, Thermal-conductivity measurements of gaas/alas superlattices using a picosecond optical pump-and-probe technique, Phys. Rev. B 59 (1999) 8105–8113, https://doi.org/10.1103/PhysRevB.59.8105. https://link.aps.org/doi/10.1103/PhysRevB.59.8105.
[137] R. Venkatasubramanian, Lattice thermal conductivity reduction and phonon localizationlike behavior in superlattice structures, Phys. Rev. B 61 (4) (2000) 3091–3097, https://doi.org/10.1103/PhysRevB.61.3091.
[138] J.-S. Wang, J. Wang, J. Lü, Quantum thermal transport in nanostructures, Euro. Phys. J. 62 (4) (2008) 381–404, https://doi.org/10.1140/epjb/e2008-00195-8.
[139] J.-S. Wang, B.K. Agarwalla, H. Li, J. Thingna, Nonequilibrium green's function method for quantum thermal transport, Front. Phy. 9 (6) (2014) 673–697, https://doi.org/10.1007/s11467-013-0340-x.
[140] C.A. Polanco, Nonequilibrium green's functions (negf) in vibrational energy transport: a topical review, Nanoscale Microscale Thermophys. Eng. 25 (1) (2021) 1–24, https://doi.org/10.1080/15567265.2021.1881193.
[141] M.N. Luckyanova, J. Garg, K. Esfarjani, A. Jandl, M.T. Bulsara, A.J. Schmidt, A.J. Minnich, S. Chen, M.S. Dresselhaus, Z. Ren, E.A. Fitzgerald, G. Chen, Coherent phonon heat conduction in superlattices, Science 338 (6109) (2012) 936–939, https://doi.org/10.1126/science.1225549.
[142] Z. Tian, K. Esfarjani, G. Chen, Green's function studies of phonon transport across Si/Ge superlattices, Phys. Rev. B 89 (23) (2014) 235307, https://doi.org/10.1103/PhysRevB.89.235307.
[143] B. Qiu, G. Chen, Z. Tian, Effects of aperiodicity and roughness on coherent heat conduction in superlattices, Nanoscale Microscale Thermophys. Eng. 19 (4) (2015) 272–278, https://doi.org/10.1080/15567265.2015.1102186.
[144] T. Ouyang, Y.P. Chen, K.K. Yang, J.X. Zhong, Thermal transport of isotopic-superlattice graphene nanoribbons with zigzag edge, Europhys. Lett. 88 (2) (2009) 28002, https://doi.org/10.1209/0295-5075/88/28002.
[145] J.W. Jiang, J.S. Wang, B.S. Wang, Minimum thermal conductance in graphene

and boron nitride superlattice, Appl. Phys. Lett. 99 (4) (2011): 043109, https://doi.org/10.1063/1.3619832.
[146] M. Luisier, Atomistic modeling of anharmonic phonon-phonon scattering in nanowires, Phys. Rev. B 86 (24) (2012) 245407, https://doi.org/10.1103/PhysRevB.86.245407.
[147] M.N. Luckyanova, J.A. Johnson, A.A. Maznev, J. Garg, A. Jandl, M.T. Bulsara, E.A. Fitzgerald, K.A. Nelson, G. Chen, Anisotropy of the thermal conductivity in gaas/alas superlattices, Nano Lett. 13 (9) (2013) 3973–3977.
[148] R. Hu, Z. Tian, Direct observation of phonon Anderson localization in Si/Ge aperiodic superlattices, Phys. Rev. B 103 (4) (2021) 45304, https://doi.org/10.1103/PhysRevB.103.045304.
[149] S. Hu, Z. Zhang, P. Jiang, J. Chen, S. Volz, M. Nomura, B. Li, Randomness-induced phonon localization in graphene heat conduction, J. Phys. Chem. Lett. 9 (14) (2018) 3959–3968, https://doi.org/10.1021/acs.jpclett.8b01653.
[150] P.W. Anderson, Absence of diffusion in certain random lattices, Phys. Rev. 109 (5) (1958) 1492–1505, https://doi.org/10.1103/PhysRev.109.1492.
[151] J. Mendoza, G. Chen, Anderson localization of thermal phonons leads to a thermal conductivity maximum, Nano Lett. 16 (12) (2016) 7616–7620, https://doi.org/10.1021/acs.nanolett.6b03550.
[152] M.N. Luckyanova, J. Mendoza, H. Lu, B. Song, S. Huang, J. Zhou, M. Li, Y. Dong, H. Zhou, J. Garlow, L. Wu, B.J. Kirby, A.J. Grutter, A.A. Puretzky, Y. Zhu, M.S. Dresselhaus, A. Gossard, G. Chen, Phonon localization in heat conduction, Sci. Adv. 4 (12) (2018): eaat9460, https://doi.org/10.1126/sciadv.aat9460.
[153] S. Volz, J.B. Saulnier, G. Chen, P. Beauchamp, Computation of thermal conductivity of Si/Ge superlattices by molecular dynamics techniques, Microelectron. J. 31 (9) (2000) 815–819, https://doi.org/10.1016/S0026-2692(00)00064-1.
[154] H. Bao, J. Chen, X. Gu, B. Cao, A review of simulation methods in micro/nanoscale heat conduction, ES Energy Envrion. 1 (2018) 16–55, https://doi.org/10.30919/esee8c149.
[155] J. Chen, G. Zhang, B. Li, Impacts of atomistic coating on thermal conductivity of germanium nanowires, Nano Lett. 12 (6) (2012) 2826–2832, https://doi.org/10.1021/nl300208c.
[156] B.C. Daly, H.J. Maris, K. Imamura, S. Tamura, Molecular dynamics calculation of the thermal conductivity of superlattices, Phys. Rev. B 66 (2) (2002): 024301, https://doi.org/10.1103/PhysRevB.66.024301.
[157] K. Imamura, Y. Tanaka, N. Nishiguchi, S. Tamura, H.J. Maris, Lattice thermal conductivity in superlattices: molecular dynamics calculations with a heat reservoir method, J. Phys. Condens. Matter 15 (50) (2003) 8679–8690, https://doi.org/10.1088/0953-8984/15/50/002.
[158] J. Chen, G. Zhang, B. Li, Tunable thermal conductivity of Si1-x Gex nanowires, Appl. Phys. Lett. 95 (7) (2009): 073117, https://doi.org/10.1063/1.3212737.
[159] M. Hu, D. Poulikakos, Si/Ge superlattice nanowires with ultralow thermal conductivity, Nano Lett. 12 (11) (2012) 5487–5494, https://doi.org/10.1021/nl301971k.
[160] X. Mu, T. Zhang, D.B. Go, T. Luo, Coherent and incoherent phonon thermal transport in isotopically modified graphene superlattices, Carbon 83 (2015) 208–216, https://doi.org/10.1016/j.carbon.2014.11.028.
[161] C. Da Silva, F. Saiz, D.A. Romero, C.H. Amon, Coherent phonon transport in short-period two-dimensional superlattices of graphene and boron nitride, Phys. Rev. B 93 (12) (2016) 125427, https://doi.org/10.1103/PhysRevB.93.125427.
[162] X. Wang, M. Wang, Y. Hong, Z. Wang, J. Zhang, Coherent and incoherent phonon transport in a graphene and nitrogenated holey graphene superlattice, Phys. Chem. Chem. Phys. 19 (35) (2017) 24240–24248, https://doi.org/10.1039/c7cp04219a.
[163] I.M. Felix, L.F.C. Pereira, Thermal conductivity of graphene-hBN superlattice ribbons, Sci. Rep. 8 (1) (2018) 2737, https://doi.org/10.1038/s41598-018-20997-8.
[164] S. Hu, Z. Zhang, P. Jiang, W. Ren, C. Yu, J. Shiomi, J. Chen, Disorder limits the coherent phonon transport in two-dimensional phononic crystal structures, Nanoscale 11 (24) (2019) 11839–11846, https://doi.org/10.1039/c9nr02548k.
[165] P. Roy Chowdhury, C. Reynolds, A. Garrett, T. Feng, S.P. Adiga, X. Ruan, Machine learning maximized Anderson localization of phonons in aperiodic superlattices, Nano Energy 69 (December 2019) (2020) 104428, https://doi.org/10.1016/j.nanoen.2019.104428.
[166] X. Wan, W. Feng, Y. Wang, H. Wang, X. Zhang, C. Deng, N. Yang, Materials discovery and properties prediction in thermal transport via materials informatics: a mini review, Nano Lett. 19 (6) (2019) 3387–3395, https://doi.org/10.1021/acs.nanolett.8b05196.
[167] S. Ju, S. Shimizu, J. Shiomi, Designing thermal functional materials by coupling thermal transport calculations and machine learning, J. Appl. Phys. 128 (16) (2020) 161102, https://doi.org/10.1063/5.0017042.
[168] J. Guo, S. Ju, J. Shiomi, Application of Bayesian Optimization to Thermal Science, 2020, https://doi.org/10.1088/978-0-7503-1738-2ch5.
[169] Y. Ouyang, C. Yu, G. Yan, J. Chen, Machine learning approach for the prediction and optimization of thermal transport properties, Front. Phy. 16 (4) (2021) 43200, https://doi.org/10.1007/s11467-020-1041-x.
[170] J. Chen, G. Zhang, B. Li, Phonon coherent resonance and its effect on thermal transport in core-shell nanowires, J. Chem. Phys. 135 (10) (2011) 104508, https://doi.org/10.1063/1.3637044.
[171] H. Honarvar, L. Yang, M.I. Hussein, Thermal transport size effects in silicon membranes featuring nanopillars as local resonators, Appl. Phys. Lett. 108 (26) (2016) 263101, https://doi.org/10.1063/1.4954739.
[172] D. Ma, H. Ding, H. Meng, L. Feng, Y. Wu, J. Shiomi, N. Yang, Nano-cross-junction effect on phonon transport in silicon nanowire cages, Phys. Rev. B 94 (16) (2016) 165434, https://doi.org/10.1103/PhysRevB.94.165434.
[173] S. Xiong, K. Sääskilahti, Y.A. Kosevich, H. Han, D. Donadio, S. Volz, Blocking phonon transport by structural resonances in alloy-based nanophononic metamaterials leads to ultralow thermal conductivity, Phys. Rev. Lett. 117 (2) (2016): 025503, https://doi.org/10.1103/PhysRevLett.117.025503.
[174] H. Honarvar, M.I. Hussein, Two orders of magnitude reduction in silicon membrane thermal conductivity by resonance hybridizations, Phys. Rev. B 97 (19) (2018) 195413, https://doi.org/10.1103/PhysRevB.97.195413.
[175] M.I. Hussein, C.N. Tsai, H. Honarvar, Thermal conductivity reduction in a nanophononic metamaterial versus a nanophononic crystal: a review and comparative analysis, Adv. Funct. Mater. 30 (8) (2020) 1906718, https://doi.org/10.1002/adfm.201906718.
[176] H. Wang, Y. Cheng, M. Nomura, S. Volz, D. Donadio, X. Zhang, S. Xiong, Synergistic impeding of phonon transport through resonances and screw dislocations, Phys. Rev. B 103 (8) (2021) 85414, https://doi.org/10.1103/PhysRevB.103.085414.
[177] H. Wang, Y. Cheng, Z. Fan, Y. Guo, Z. Zhang, M. Bescond, M. Nomura, T. Ala-Nissila, S. Volz, S. Xiong, Anomalous thermal conductivity enhancement in low dimensional resonant nanostructures due to imperfections, Nanoscale 13 (22) (2021) 10010–10015, https://doi.org/10.1039/d1nr01679b.
[178] S. Pailhès, H. Euchner, V.M. Giordano, R. Debord, A. Assy, S. Gomès, A. Bosak, D. Machon, S. Paschen, M. De Boissieu, Localization of propagative phonons in a perfectly crystalline solid, Phys. Rev. Lett. 113 (2) (2014): 025506, https://doi.org/10.1103/PhysRevLett.113.025506.
[179] Q. Xi, Z. Zhang, T. Nakayama, J. Chen, J. Zhou, B. Li, Off-center rattling triggers high-temperature thermal transport in thermoelectric clathrates: non-perturbative approach, Phys. Rev. B 97 (22) (2018) 224308, https://doi.org/10.1103/PhysRevB.97.224308.
[180] C. Chen, Z. Zhang, J. Chen, Revisit to the impacts of rattlers on thermal conductivity of clathrates, Front. Energy Res. 6 (MAY) (2018) 34, https://doi.org/10.3389/fenrg.2018.00034.
[181] D. Ma, X. Wan, N. Yang, Unexpected thermal conductivity enhancement in pillared graphene nanoribbon with isotopic resonance, Phys. Rev. B 98 (24) (2018) 245420, https://doi.org/10.1103/PhysRevB.98.245420.
[182] Z. Zhang, J. Chen, B. Li, Negative Gaussian curvature induces significant suppression of thermal conduction in carbon crystals, Nanoscale 9 (37) (2017) 14208–14214, https://doi.org/10.1039/c7nr04944g.
[183] Z. Zhang, S. Hu, T. Nakayama, J. Chen, B. Li, Reducing lattice thermal conductivity in schwarzites via engineering the hybridized phonon modes, Carbon 139 (2018) 289–298, https://doi.org/10.1016/j.carbon.2018.06.057.
[184] Z. Zhang, Y. Ouyang, J. Chen, S. Volz, A phononic rectifier based on carbon schwarzite host-guest system, Chin. Phys. B 29 (12) (2020) 124402, https://doi.org/10.1088/1674-1056/abbbf9.
[185] Z. Zhang, S. Hu, Q. Xi, T. Nakayama, S. Volz, J. Chen, B. Li, Tunable phonon nanocapacitor built by carbon schwarzite based host-guest system, Phys. Rev. B 101 (8) (2020): 081402, https://doi.org/10.1103/PhysRevB.101.081402. R).
[186] Y. Wang, H. Huang, X. Ruan, Decomposition of coherent and incoherent phonon conduction in superlattices and random multilayers, Phys. Rev. B 90 (16) (2014) 165406, https://doi.org/10.1103/PhysRevB.90.165406.
[187] Z. Zhang, Y. Guo, M. Bescond, J. Chen, M. Nomura, S. Volz, Generalized decay law for particlelike and wavelike thermal phonons, Phys. Rev. B 103 (18) (2021) 184307, https://doi.org/10.1103/PhysRevB.103.184307.
[188] A.M. Marconnet, T. Kodama, M. Asheghi, K.E. Goodson, Phonon conduction in periodically porous silicon nanobridges, Nanoscale Microscale Thermophys. Eng. 16 (4) (2012) 199–219, https://doi.org/10.1080/15567265.2012.732195.
[189] R. Anufriev, R. Yanagisawa, M. Nomura, Aluminium nanopillars reduce thermal conductivity of silicon nanobeams, Nanoscale 9 (39) (2017) 15083–15088, https://doi.org/10.1039/C7NR05114J.
[190] K. Celebi, J. Buchheim, R.M. Wyss, A. Droudian, P. Gasser, I. Shorubalko, J.-I. Kye, C. Lee, H.G. Park, Ultimate permeation across atomically thin porous graphene, Science 344 (6181) (2014) 289–292, https://doi.org/10.1126/science.1249097.
[191] X. Zianni, The effect of the modulation shape in the ballistic thermal conductance of modulated nanowires, J. Solid State Chem. 193 (2012) 53–57, https://doi.org/10.1016/j.jssc.2012.03.066.
[192] K. Termentzidis, T. Barreteau, Y. Ni, S. Merabia, X. Zianni, Y. Chalopin, P. Chantrenne, S. Volz, Modulated SiC nanowires: molecular dynamics study of their thermal properties, Phys. Rev. B 87 (12) (2013) 125410, https://doi.org/10.1103/PhysRevB.87.125410.
[193] X. Zianni, V. Jean, K. Termentzidis, D. Lacroix, Scaling behavior of the thermal conductivity of width-modulated nanowires and nanofilms for heat transfer control at the nanoscale, Nanotechnology 25 (46) (2014) 465402, https://doi.org/10.1088/0957-4484/25/46/465402.
[194] R. Anufriev, M. Nomura, Heat conduction engineering in pillar-based phononic crystals, Phys. Rev. B 95 (15) (2017) 155432, https://doi.org/10.1103/PhysRevB.95.155432.
[195] R. Anufriev, M. Nomura, Coherent thermal conduction in silicon nanowires with periodic wings, Nanomaterials 9 (2) (2019) 142, https://doi.org/10.3390/nano9020142.
[196] R. Anufriev, S. Gluchko, S. Volz, M. Nomura, Quasi-ballistic heat conduction

due to lévy phonon flights in silicon nanowires, ACS Nano 12 (2018) 11928–11935, https://doi.org/10.1021/acsnano.8b07597.
[197] C. Blanc, A. Rajabpour, S. Volz, T. Fournier, O. Bourgeois, Phonon heat conduction in corrugated silicon nanowires below the Casimir limit, Appl. Phys. Lett. 103 (4) (2013): 043109, https://doi.org/10.1063/1.4816590 arXiv:arXiv:1302.4422v1.
[198] V. Poborchii, Y. Morita, J. Hattori, T. Tada, P.I. Geshev, Corrugated Si nanowires with reduced thermal conductivity for wide-temperature-range thermoelectricity, J. Appl. Phys. 120 (2016) 154304, https://doi.org/10.1063/1.4965302.
[199] S. Xiong, K. Sääskilahti, Y.a. Kosevich, H. Han, D. Donadio, S. Volz, Blocking phonon transport by structural resonances in alloy-based nanophononic metamaterials leads to ultralow thermal conductivity, Phys. Rev. Lett. 117 (2) (2016): 025503, https://doi.org/10.1103/PhysRevLett.117.025503.
[200] A. Iskandar, A. Gwiazda, Y. Huang, M. Kazan, A. Bruyant, M. Tabbal, G. Lerondel, Modification of the phonon spectrum of bulk Si through surface nanostructuring, J. Appl. Phys. 120 (9) (2016): 095106, https://doi.org/10.1063/1.4962208.
[201] B. Graczykowski, M. Sledzinska, F. Alzina, J. Gomis-Bresco, J.S. Reparaz, M.R. Wagner, C.M. Sotomayor Torres, Phonon dispersion in hypersonic two-dimensional phononic crystal membranes, Phys. Rev. B 91 (7) (2015): 075414, https://doi.org/10.1103/PhysRevB.91.075414.
[202] M.R. Wagner, B. Graczykowski, J.S. Reparaz, A. El Sachat, M. Sledzinska, F. Alzina, C.M. Sotomayor Torres, Two-dimensional phononic crystals: disorder matters, Nano Lett. 16 (9) (2016) 5661–5668, https://doi.org/10.1021/acs.nanolett.6b02305, arXiv:1511.07398.
[203] R. Anufriev, S. Tachikawa, S. Gluchko, Y. Nakayama, T. Kawamura, L. Jalabert, M. Nomura, Cross-plane thermal conductivity in amorphous Si/SiO 2 superlattices, Appl. Phys. Lett. 117 (9) (2020): 093103, https://doi.org/10.1063/5.0023782.
[204] Y. Liao, S. Iwamoto, M. Sasaki, M. Goto, J. Shiomi, Heat conduction below diffusive limit in amorphous superlattice structures, Nano Energy 84 (December 2020) (2021) 105903, https://doi.org/10.1016/j.nanoen.2021.105903.
[205] E. Chavez-Angel, N. Reuter, P. Komar, S. Heinz, U. Kolb, H.-J. Kleebe, G. Jakob, Subamorphous thermal conductivity of crystalline half-heusler superlattices, Nanoscale Microscale Thermophys. Eng. 23 (1) (2019) 1–9, https://doi.org/10.1080/15567265.2018.1505987.
[206] P. Hołuj, C. Euler, B. Balke, U. Kolb, G. Fiedler, M.M. Müller, T. Jaeger, E. Chávez Angel, P. Kratzer, G. Jakob, Reduced thermal conductivity of TiNiSn/HfNiSn superlattices, Phys. Rev. B 92 (12) (2015) 125436, https://doi.org/10.1103/PhysRevB.92.125436.
[207] B. Saha, Y.R. Koh, J.P. Feser, S. Sadasivam, T.S. Fisher, A. Shakouri, T.D. Sands, Phonon wave effects in the thermal transport of epitaxial TiN/(Al,Sc)N metal/semiconductor superlattices, J. Appl. Phys. 121 (1) (2017): 015109, https://doi.org/10.1063/1.4973681.
[208] G. Arregui, O. Ortíz, M. Esmann, C.M. Sotomayor-Torres, C. Gomez-Carbonell, O. Mauguin, B. Perrin, A. Lemaître, P.D. García, N.D. Lanzillotti-Kimura, Coherent generation and detection of acoustic phonons in topological nanocavities, APL Photon. 4 (3) (2019): 030805, https://doi.org/10.1063/1.5082728 arXiv:1811.09781.
[209] M. Maldovan, Narrow low-frequency spectrum and heat management by thermocrystals, Phys. Rev. Lett. 110 (2) (2013): 025902, https://doi.org/10.1103/PhysRevLett.110.025902.
[210] T. Kodama, M. Ohnishi, W. Park, T. Shiga, J. Park, T. Shimada, H. Shinohara, J. Shiomi, K.E. Goodson, Modulation of thermal and thermoelectric transport in individual carbon nanotubes by fullerene encapsulation, Nat. Mater. 16 (9) (2017) 892–897, https://doi.org/10.1038/nmat4946.
[211] C. Dames, Ultrahigh thermal conductivity confirmed in boron arsenide, Science 361 (6402) (2018) 549–550, https://doi.org/10.1126/science.aau4793.
[212] J.S. Kang, M. Li, H. Wu, H. Nguyen, Y. Hu, Experimental observation of high thermal conductivity in boron arsenide, Science 361 (6402) (2018) 575–578, https://doi.org/10.1126/science.aat5522.
[213] F. Tian, B. Song, X. Chen, N.K. Ravichandran, Y. Lv, K. Chen, S. Sullivan, J. Kim, Y. Zhou, T.-H. Liu, M. Goni, Z. Ding, J. Sun, G.A.G. Udalamatta Gamage, H. Sun, H. Ziyaee, S. Huyan, L. Deng, J. Zhou, A.J. Schmidt, S. Chen, C.-W. Chu, P.Y. Huang, D. Broido, L. Shi, G. Chen, Z. Ren, Unusual high thermal conductivity in boron arsenide bulk crystals, Science 361 (6402) (2018) 582–585, https://doi.org/10.1126/science.aat7932.
[214] S. Li, Q. Zheng, Y. Lv, X. Liu, X. Wang, P.Y. Huang, D.G. Cahill, B. Lv, High thermal conductivity in cubic boron arsenide crystals, Science 361 (6402) (2018) 579–581, https://doi.org/10.1126/science.aat8982.
[215] K. Chen, B. Song, N.K. Ravichandran, Q. Zheng, X. Chen, H. Lee, H. Sun, S. Li, G.A.G. Udalamatta Gamage, F. Tian, Z. Ding, Q. Song, A. Rai, H. Wu, P. Koirala, A.J. Schmidt, K. Watanabe, B. Lv, Z. Ren, L. Shi, D.G. Cahill, T. Taniguchi, D. Broido, G. Chen, Ultrahigh thermal conductivity in isotope-enriched cubic boron nitride, Science 367 (6477) (2020) 555–559, https://doi.org/10.1126/science.aaz6149.
[216] X. Li, S. Ning, Z. Liu, Z. Yan, C. Luo, Z. Zhuang, Designing phononic crystal with anticipated band gap through a deep learning based data-driven method, Comput. Methods Appl. Mech. Eng. 361 (2020) 112737, https://doi.org/10.1016/j.cma.2019.112737. https://www.sciencedirect.com/science/article/pii/S0045782519306279.
[217] S.M. Sadat, R.Y. Wang, A machine learning based approach for phononic crystal property discovery, J. Appl. Phys. 128 (2) (2020): 025106, https://doi.org/10.1063/5.0006153 arXiv:.
[218] X.-B. Miao, H.W. Dong, Y.-S. Wang, Deep learning of dispersion engineering in two-dimensional phononic crystals, 0 (0), Eng. Optim. (2021) 1–15, https://doi.org/10.1080/0305215X.2021.1988587. arXiv.
[219] K. Ren, X. Liu, S. Chen, Y. Cheng, W. Tang, G. Zhang, Remarkable reduction of interfacial thermal resistance in nanophononic heterostructures, Adv. Funct. Mater. 30 (42) (2020) 2004003, https://doi.org/10.1002/adfm.202004003.
[220] H. Wang, S. Hu, K. Takahashi, X. Zhang, H. Takamatsu, J. Chen, Experimental study of thermal rectification in suspended monolayer graphene, Nat. Commun. 8 (May) (2017) 1–8, https://doi.org/10.1038/ncomms15843.